N93-30848

COMPARISON OF IMPACT RESULTS FOR SEVERAL POLYMERIC COMPOSITES OVER A WIDE RANGE OF LOW IMPACT VELOCITIES

C. C. Poe, Jr.
NASA Langley Research Center
Hampton, VA

M. A. Portanova
and
J. E. Masters
Lockheed Engineering and Sciences Co.
Hampton, VA

B. V. Sankar
University of Florida
Gainesville, FL

Wade C. Jackson
U.S. Army Aerostructures Directorate, USAARTA-AVSCOM
Hampton, VA

SUMMARY

Static indentation, falling weight, and ballistic impact tests were conducted on clamped plates made of AS4/3501-6 and IM7/8551-7 prepreg tape. The transversely isotropic plates were nominally 7-mm thick. Pendulum and ballistic tests were also conducted on simply supported plates braided with Celion 12000 fibers and 3501-6 epoxy. The 20^{0} braided plates were about 5-mm thick. The impacters had spherical or hemispherical shapes with a 12.7 mm diameter. Residual compression strength and damage size were measured. Except for the ballistic tests, impact force was measured. An impact analysis was conducted using plate equations to aid in understanding the experimental results.

For a given kinetic energy, damage size was least for IM7/8551-7 and greatest for the braided material. Strengths varied inversely with damage size. For a given damage size, strength loss as a fraction of original strength was least for the braided material and greatest for AS4/3501-6 and IM7/8551-7. Strength loss for IM7/8551-7 and AS4/3501-6 was nearly equal. No significant differences were noticed between damage sizes and residual compression strengths for the static indentation, falling weight, and ballistic tests of AS4/3501-6 and IM7/8551-7. For the braided material, on the other hand, sizes of damage were significantly less and compression strengths were significantly more for the falling weight tests than for the ballistic tests. The impact analysis revealed that the response to static indentation and falling weight tests should

be essentially the same for the same boundary conditions, but that ballistic tests are more severe than static indentation and falling weight tests when plates are simply supported but not necessarily when plates are clamped.

INTRODUCTION

Low-velocity impacts from dropped tools, falling equipment, runway debris and hail can cause damage to conventional carbon-reinforced-plastics that reduce tension and compression strength by as much as two-thirds. (See for example [1-7].) Strength can even be reduced significantly without the impact damage being visible on the surface. In a very thick AS4 laminate wet-wound with a conventional epoxy, the impact damage from hemispherical indenters initiated at a contact pressure of 500 MPa, but the damage was not in evidence on the surface until the pressure exceeded 700 MPa [5]. The damage, which consisted of translaminar matrix cracks and broken fibers, initiated just below the contact site and did not spread much beyond the contact region. In thin epoxy laminates, the damage can initiate at a lower pressure, and delaminations can also develop and extend far beyond the contact region. Compression strengths are also reduced by delaminations, which cause sublaminates to buckle and overload the remainder of the laminate. In most structural metals, a 500 MPa contact pressure would only cause local yielding and no strength loss.

The impact damage was also successfully predicted in [5]. An energy balance model was used to predict impact force and a quasi-static stress analysis, and maximum shear stress criterion was used to predict damage for the contact problem. Impact damage was predicted to be independent of impacter mass and velocity as long as the kinetic energy was a constant and the impacter mass was small relative to that of the target.

For thin laminates, Elber proposed that static indentation tests, which are simple to conduct, can be equivalent to falling weight or pendulum impact tests [8]. In a static indentation test, the impact is simulated by a quasi-static application of a transverse load through an indenter or tup of desired shape.

In addition to falling weight and static indentation tests, impact tests have also been conducted using swinging pendulums and gas guns. The velocity and mass for the pendulum and falling weight tests are similar because both rely upon gravity. On the other hand, velocities for the gas gun tests, hereafter called ballistic tests, can be more than an order of magnitude times those of falling weight tests. Yet falling weight and ballistic tests are both called "low velocity" impact tests.

Comparisons between ballistic and falling weight tests of tape laminates in [2] indicate that residual compression strengths were less for ballistic tests than for falling weight tests for a given kinetic energy. Ballistic tests were also shown to be more severe than falling weight tests in [6,7]. For a given kinetic energy, delamination area was larger and residual tension strengths were smaller for ballistic tests than for falling weight tests. Also, the energy threshold for penetration was smaller for ballistic tests than for falling weight tests.

During impact, the specimens in [2] were simply supported on the long sides and clamped on the short sides, and those in [6,7] were free on the long sides and clamped on the short sides. However, circular plates clamped on the edges were also tested in [7]. For 8-ply tape laminates, the residual tension strengths for ballistic tests were less than those for falling weight tests. For 16-ply laminates, on the other hand, tension strengths were about equal for ballistic and falling weight tests. Thus, thickness and boundary conditions appear to have a significant effect on the outcome of impact tests.

Thus, published results indicate that, even when kinetic energy is fixed, impact response can differ between falling weight and ballistic tests. Energy balance models and quasi-static stress analyses such as those in [5] may be accurate for falling weight tests where impacter velocities are relatively low but may not be accurate for ballistic tests where velocities are relatively large. Accordingly, experiments were conducted to quantify differences between impact damage and residual compression strength for static indentation, falling weight, pendulum, and ballistic impact tests. A braided material and two tape laminates (one made with a brittle epoxy and one made with a toughened epoxy) were tested. The 48 ply, transversely isotropic tape laminates have been used as a standard by NASA for determining damage tolerance allowables for toughened and untoughened composites. Analyses were also conducted to develop an understanding of the impact response for varying impacter mass and velocity. The analyses were conducted for a simply supported anisotropic plate using plate theory with local indentation represented by Hertzian contact [9]. The plate theory takes into account the higher mode shapes that are important for high velocity impacts like those in the ballistic tests.

SYMBOLS

Values are given in SI Units. Measurements were made in U.S. Customary Units.

A_{11}, A_{22}, A_{12}	constants in Hertz's equation, Pa
E_1	Young's modulus of isotropic impacter, Pa
E_r, E_z	Young's moduli of transversely, isotropic plate, Pa
F_{max}	impact force, N
G_{zr}	shear modulus of transversely, isotropic plate, Pa
k_1, k_2	constants in Hertz's equation, Pa
k_b	spring constant for plate, N/m
KE_{eff}	effective kinetic energy, J
M	effective mass, kg
m_1, m_2	mass of impacter and plate, respectively, kg
n_0	constant in Hertz's equation, Pa
r_c	contact radius, m
R_i	radius of spherical impacter, m

v_1	velocity of impacter, m/s
α	αm_2 is the effective mass of the plate
ν_1	Poisson's ratio of isotropic impacter
ν_r, ν_{rz}	Poisson's ratio of transversely, isotropic plate
Subscripts:	
r,z	cylindrical coordinates (The z-direction is normal to the plate.)

EXPERIMENTS

Materials

The stacking sequence of the 48-ply IM7/8551-7 and AS4/3501-6 tape laminates was $[45/0/-45/90]_{6S}$. The fracture toughness (mode I strain energy release rate) of 8551-7 epoxy is significantly greater than that of 3501-6 epoxy [10]. The thickness of the tape laminates was 7.0 mm, and the fiber volume fractions were 0.547 and 0.567 for the IM7/8551-7 and AS4/3501-6 laminates, respectively. The undamaged compression strength of IM7/8551-7 laminates with the same layup was reported to be 620 MPa in [4,11], and the undamaged compression strength of an AS4/3501-6 laminate with the same layup but made with uniweave fabric and resin transfer molding was 586 MPa [12].

The Celion 12000 braided material was impregnated with 3501-6 epoxy. The epoxy was introduced into the braided fiber using a resin transfer molding process. The braid pattern was 1x1x1, the braid angle was about 20^{0}, and the thickness of the cured plates varied from 5.8 mm on the edges to 4.8 mm in the center. The fiber volume fraction was 0.60 with 2 percent void. The undamaged compression strength was 156 MPa, which is less than one-half that of similar braided materials [13]. The reason for the lower strengths was not evident.

Test Procedures

Tape Laminates.- Static indentation, falling weight, and ballistic impact tests were conducted at NASA Langley Research Center on the plates made with AS4/3501-6 and IM7/8551-7 prepreg tape. Contact diameters were measured by placing a sheet of white bond paper on the front surface of the plate and a sheet of carbon paper on top of the white bond paper. Contact by the impacter caused carbon to transfer to the white paper. The diameter of carbon on the white paper was assumed to equal the contact diameter. Following impact, an ultrasonic C-scan map was made of each plate, and the size of the damaged area was measured. Then the plates were loaded to failure in uniaxial compression in a fixture that simply supported the free edges to prevent global buckling. The loading direction was parallel to the long dimension of the plates.

For the static indentation tests, 12.7- by 12.7-cm square composite plates were clamped to a metal plate containing a circular hole with a diameter of 10.2 cm. A servo-controlled testing machine was used to apply the monotonically increasing contact force at the center of the opening. A steel hemisphere with 12.7-mm diameter was used for an indenter or tup. See figure 1.

For the falling weight and ballistic impact tests, rectangular composite plates 17.8 by 25.4 cm were clamped to a metal plate containing a 12.7- by 12.7-cm square opening [4]. The impacts were centered on the opening. The width of the plates was trimmed from 17.8 to 12.7 cm before the plates were loaded to failure. See figure 2.

The falling weight impacter had a mass of 4.63 kg and was instrumented to measure impact force. A steel hemisphere with 12.7-mm diameter was attached to the end of the impacter for an indenter. The velocities ranged from 1.71 to 5.14 m/s, and the kinetic energies ranged from 6.78 to 61.0 J.

A gas gun was used for the ballistic impact tests. A 3.00-g, 12.7-mm-dia. aluminum sphere was used for the impacter. The velocities ranged from 67.8 to 160 m/s, and the kinetic energies ranged from 6.78 to 37.7 J.

One AS4/3501-6 specimen (D05A) and one IM7/8551-7 specimen (D05IR) impacted with the falling weight and one AS4/3501-6 specimen (D15A) impacted with the gas gun were sectioned through the impact site. The sections were polished and edge replicas were made of the polished sections using a cellulose acetate film. The edge replicas were examined to reveal the pattern of damage. The portions of plates that were not polished were pyrolized to reveal broken fibers in the individual plies. The kinetic energy for all three specimens was 27.1 J.

Braided material.- Pendulum and ballistic impact tests were conducted at the University of Florida on plates made with the braided material. The square plates were 10.2 by 10.2 cm and simply supported on all sides. Following impact, the plates were radiographed and damage sizes were measured. Then the plates were trimmed to a size of 7.62 by 7.62 cm and loaded uniaxially in compression in a fixture that simply supported the free edges to prevent global buckling. See figure 3.

For the pendulum tests, a steel hemisphere with 12.7-mm diameter was attached to the end of the impacter for an indenter. The mass of the pendulum was 13.84 kg, the velocities ranged from 1.42 to 2.68 m/s, and the values of kinetic energy ranged from 14.0 to 49.9 J. The pendulum was instrumented to measure impact force.

A gas gun was used for the ballistic tests. A steel rod with a diameter of 12.7 mm, a length of 15.9 mm, and a hemispherical end was used for the impacter. The mass of the impacter was 0.0145 kg, the velocities ranged from 43.2 to 86.3 m/s, and the values of kinetic energy ranged from 13.5 to 54.0 J.

Results

Impact parameters, impact force, damage size (area), and compression strength for each test are given in Tables I and II for the AS4/3501-6 and IM7/8551-7 laminates, respectively, and in Table III for the braided material. Contact diameters, descriptions of the damage visible on front and back faces, and the maximum depth of broken fibers in the deplied specimens (D05A, D15A, and D05IR) are also given in Tables I and II.

The approach used in presenting the results is to first compare static indentation and falling weight test results for a given impact force, then to

compare falling weight (or pendulum) and ballistic impact test results for a given kinetic energy, and finally to compare residual strengths for a given damage size determined from nondestructive examinations. No static indentation results are available for the braided material.

Impact damage.- The damage size is plotted against impact force for the static indentation and falling weight impact tests in figure 4(a) for AS4/3501-6 and figure 4(b) for IM7/8551-7. As in subsequent figures of experimental results, lines were drawn through the data to show trends. The area of damage increases with increasing impact force and is much smaller for IM7/8551-7 than AS4/3501-6 for a given impact force. The damage sizes for the static and falling weight impact tests agree quite well for both AS4/3501-6 and IM7/8551-7. Both materials exhibit an impact force threshold for initiating damage. The threshold is larger for IM7/8551-7 than for AS4/3501-6.

The damage size is plotted against kinetic energy for the ballistic and falling weight impact tests in figure 5(a) for AS4/3501-6 and figure 5(b) for IM7/8551-7. The vertical lines correspond to an industry standard of 6.67 J/mm thickness (1500 in-lbf/in thickness) [14]. Damage size increases with increasing kinetic energy. For AS4/3501-6 in figure 5(a), the damage sizes were somewhat larger for the falling weight tests than for the ballistic tests for a given kinetic energy; and, for IM7/8551-7 in figure 5(b), the damage sizes for the falling weight and ballistic tests were equal. For a given kinetic energy, damage sizes were much less for IM7/8551-7 than for AS4/3501-6. Much as the impact force threshold in Figs. 4(a) and 4(b), the kinetic energy threshold for initiating damage in Figs. 5(a) and 5(b) is larger for IM7/8551-7 than for AS4/3501-6. The aluminum spheres that were used as impacters in the ballistic tests permanently deformed for kinetic energies of 20.3 to 27.1 J and greater.

The undulations in the data in figure 5(a) give an appearance of large scatter. However, the difference between duplicate tests for kinetic energies of 13.6 and 27.1 J is relatively small. (Each symbol represents one test.)

The values of impact force and kinetic energy at which damage became visible on the front and back faces are also shown in Figs. 4 and 5. Damage becomes visible on the front face at a lower impact force and kinetic energy than on the back face. On the front face, damage is visible first as a dent. The dent increases in size and depth with increasing impact force and kinetic energy, and eventually fibers are broken in the dent. Except for the static indentation tests, damage is visible on the back face first as a bump. The bump is opposite the dent on the front face, indicating through-the-thickness damage. Like the dent on the front face, the bump on the back face increases in size and height with increasing kinetic energy and impact force, and eventually fibers are broken on the bump. There was no significant difference between the values of kinetic energy for damage to become visible on the front and back faces for the falling weight and ballistic tests. For the static indentation test, however, no broken fibers were observed on the front face and no damage was observed on the back face before the indenter penetrated the laminate. With regard to material effect, somewhat larger values of impact force and kinetic energy were required for damage to become visible on the faces of IM7/8551-7 than on those of AS4/3501-6. Thresholds for visible damage in the C-scans were also larger for IM7/8551-7 than for AS4/3501-6.

Photographs of an edge replica for specimen D05A (falling weight test) and for specimen D15A (ballistic test) is shown in figure 6(a) and 6(b), respectively. Both specimens are AS4/3501-6 and were impacted with a kinetic energy of 27.1 J. Large delaminations were observed at each of the eleven -45/0 ply interfaces in each specimen and transverse matrix cracks were observed in most of the plies within this region. However, the patterns of damage differed as follows: 1. The delaminations were larger for the falling weight test than for the ballistic test, as evidenced in the C-scans. See figure 5(a). 2. For the ballistic test, a damage free zone extends from the front face to the laminate midplane. But, for the falling weight test, delaminations and transverse matrix cracks are present in this same zone. 3. The distribution of translaminar cracking is conical for the falling weight test and more cylindrical for the ballistic test.

Examination of the deplied sections of specimen D05A in figure 6(a) for the falling weight test revealed that only the top nine plies of the front face contained broken fibers. On the other hand, no broken fibers were found in the deplied sections of specimen D15A in figure 6(b) for the ballistic test.

A photograph of an edge replica for the IM7/8551-7 specimen impacted with a kinetic energy of 27.1 J is shown in figure 7 for the falling weight test. Delaminations were observed at each of the eleven -45/0 ply interfaces similar to the AS4/3501-6 specimens in Figs. 6(a) and 6(b). However, the delaminations were much smaller for the IM7/8551-7 specimen than the AS4/3501-6 specimens, as evidenced by the C-scan areas in figure 5(b). Also, the number of translaminar cracks is much less in the IM7/8551-7 specimen than in the AS4/3501-6 specimens. The pattern of cracks is similar to that of AS4/3501-6 in figure 6(a). Examination of the deplied section revealed that broken fibers were limited to the top three plies of the front face compared to the top nine plies of the AS4/3501-6 specimen in figure 6(a).

The damage size is plotted against kinetic energy for the ballistic and pendulum impact tests of the braided material in figure 8. The vertical line corresponds to an industry standard of 6.67 J/mm thickness (1500 in-lbf/in thickness) [14]. Damage size increases with increasing kinetic energy and, in contrast to AS4/3501-6, was less for the pendulum tests than for the ballistic tests. Damage sizes for the ballistic tests of the braided material were larger than those for the tape materials for a given kinetic energy. Notice that the damage size scale for the braided material is two times that for the tape laminates. The damage sizes for the braided material were associated with disbonded yarns. However, the disbonds did not form a continuous plane as in the case of laminates made from tape.

Residual strength.- The residual compression strengths for the static indentation and falling weight tests are plotted against impact force in figure 9(a) for AS4/3501-6 and in figure 9(b) for IM7/8551-7. For both materials, the strengths are in good agreement for a given value of impact force. The strength of AS4/3501-6 drops precipitously at the threshold for damage initiation, about 6 J in figure 4(a), whereas the strength of IM7/8551-7 in figure 9(b) decreases more gradually. The undamaged compression strengths, which are also plotted in Figs. 9(a) and 9(b), appear to be somewhat larger than those indicated by extrapolating the test data.

The residual compression strength is plotted against kinetic energy for the falling weight and ballistic tests in figure 10(a) for AS4/3501-6 and in figure 10(b) for IM7/8551-7. For AS4/3501-6, the compression strengths for a given kinetic energy were equal except for the lowest energies where the strengths were somewhat less for the falling weight tests than the ballistic tests. For IM7/8551-7, strengths for the falling weight and ballistic tests agree quite well. For the kinetic energies that correspond to the industry standard, the impacts reduced compression strength of AS4/3501-6 by about 70 percent and that of IM7/8551-7 by about 60 percent. The corresponding strength of IM7/8551-7 was about 2 times that of AS4/3501-6. Much as in Figs. 9(a) and 9(b), the undamaged compression strengths for the tape laminates in Figs. 10(a) and 10(b), appear to be somewhat larger than those indicated by extrapolating the test data.

The residual compression strength is plotted against kinetic energy in figure 11 for the pendulum and ballistic tests of the braided material. For a given value of kinetic energy, strengths are lower for the ballistic tests than the pendulum tests. For the kinetic energy that corresponds to the industry standard, the impacts reduced the compression strength by about 20 or 30 percent, depending on type of test. The corresponding strengths are about equal to that of AS4/3501-6 in figure 10(a) and about half that of IM7/8551-7 in figure 10(b).

The residual compression strength is plotted against damage size in Figs. 12(a) and 12(b) for AS4/3501-6 and IM7/8551-7, respectively. Results are shown for the static indentation, falling weight, and ballistic impact tests. The strengths decrease with increasing damage size, and all three types of tests are in reasonable agreement for a given damage size, somewhat better for IM7/8551-7 than AS4/3501-6. For a given damage size, the strengths for both tape laminates are nearly equal.

The residual compression strength is plotted against damage size in figure 13 for the pendulum and ballistic impact tests of the braided material. The strengths decrease with increasing damage size but not as precipitously as those of the tape laminates in Figs. 12(a) and 12(b). The strengths were lower for the pendulum tests than for the ballistic tests for a given damage size.

Back-face strain.- The back-face tension strain is plotted against contact force in figure 14 for a static indentation test (ST01IR) and a falling weight test (D01IR) of IM7/8551-7 specimens. The data for the falling weight test is somewhat erratic because of noise in the impact force signal. These two tests were selected because the maximum values of contact force are essentially equal. The area between the loading and unloading curves (hysteresis) is larger for the static indentation test than the falling weight test, indicating more damage in the static indentation test than in the falling weight test. Indeed, the C-scan maps indicated damage in specimen ST01IR but not in specimen D01IR. See Table II. The strains during loading of specimens D01IR and ST01IR agree below a force of 6 kN. Above a force of 6 kN, the strains for specimen ST01IR are greater than those for specimen D01IR. The initiation of delaminations at a force of 6 kN in specimen ST01IR would cause the response in figure 14.

The back-face strain is plotted against time in figure 15 for a falling weight test (D01IR) and a ballistic test (D19IP) of IM7/8551-7 specimens. The kinetic energy for both tests was 6.78 J. The maximum back-face strain, which is tension, is larger for the falling weight test than the ballistic test.

Also, the duration of the impact for the falling weight test is much larger than that for the ballistic test. For kinetic energies greater than 27.1 J, the output of strain gages was affected by back-face damage; and, for ballistic tests with kinetic energies greater than 13.6 J, strain gages separated from the specimens.

Contact diameter.- Contact diameter is plotted against impact force in figure 16 for static indentation and falling weight tests of AS4/3501-6 and IM7/8551-7 laminates. For the tests with penetration, the indenter diameter was plotted for the contact diameter. Contact diameters are in agreement except for the highest impact forces near penetration. The contact force to penetrate IM7/8551-7 was about 33 percent greater than that to penetrate AS4/3501-6. In the falling weight tests, the impact forces were not quite large enough to penetrate either laminate. Extrapolation of the falling weight test data indicate that the impact force associated with penetration for the static indentation and falling weight tests are similar.

Contact diameter is plotted against kinetic energy in figure 17 for the falling weight and ballistic tests of AS4/3501-6 and IM7/8551-7. Penetration did not occur for any of these tests. The contact diameters for the ballistic tests are significantly greater than those for the falling weight tests.

ANALYSIS

From energy balance considerations [5], the impact force F_{max} for a transversely isotropic plate is given by

$$0.4\ R_1^{-1/3}\ n_0^{-2/3}\ F_{max}^{5/3} + 0.5\ k_b^{-1}\ F_{max}^2 - KE_{eff} = 0 \tag{1}$$

where k_b is the spring constant for plate type displacements.

The term KE_{eff} is the effective kinetic energy defined by

$$KE_{eff} = 0.5\ M\ v_1^2 \tag{2}$$

where M is the effective mass defined by

$$M = [m_1^{-1} + (\alpha m_2)^{-1}]^{-1} \tag{3}$$

and v_1 and m_1 are the velocity and mass of the impacter, respectively, and m_2 and αm_2 are the mass and effective mass of the target, respectively. For a ring, $\alpha = 0.25$ was determined experimentally [5]. For a simply supported or clamped plate, α is probably greater than 0.25.

The term n_0, which is associated with Hertzian indentation, is given by

$$n_o = 4\ (k_1 + k_2)^{-1}/3 \tag{4}$$

where

$$k_1 = (1 - \nu_1^2)\ E_1^{-1} \tag{5}$$

$$k_2 = 0.5\ (A_{22}/G_{zr})^{1/2}\ (A_{11}A_{22} - A_{12}^2)^{-1}\ \{[(A_{11}A_{22})^{1/2} + G_{zr}]^2 - [A_{12} + G_{zr}]^2\}^{1/2} \tag{6}$$

$$A_{11} = E_z\ \{1 - 2\ \nu_{rz}^2\ E_z\ [E_r\ (1 - \nu_r)]^{-1}\}^{-1} \tag{7}$$

$$A_{22} = A_{11}\ (E_r\ E_z^{-1} - \nu_{rz}^2)(1 - \nu_r^2)^{-1} \tag{8}$$

and

$$A_{12} = A_{11}\ \nu_{rz}(1 - \nu_r)^{-1} \tag{9}$$

The E_1 and ν_1 are the elastic constants of the isotropic, spherical impacter. The E_r, E_z, G_{zr}, ν_r, and ν_{rz} are the elastic constants of the transversely isotropic plate in polar coordinates.

The parameters α, k_b, and n_o will vary with plate configuration and material. If the plate configuration and material are fixed, the impact force calculated with equations (1)-(9) will be constant for a given value of KE_{eff}. Otherwise, the impact force will increase with KE_{eff} to a power between 0.5 and 0.6, depending on whether or not Hertzian indentation is large or small compared to the plate deflection.

Sankar, et al solved the governing equations for impact of a simply supported anisotropic plate assuming classical plate theory [15] and, more recently, assuming plate theory with shear deformation [9]. The local indentation of the contact region was represented by Hertzian contact. In order to develop an understanding of the effects of impacter velocity and mass, the equations in [9] for a simply supported plate were solved. Contact force, back-face strain, and displacements were calculated. The displacements were calculated at the center of the plate, and the back-face strain was calculated at the center of the plate and midway between the edge and center. The plate was assumed to be 12.7- by 12.7-mm and made of AS4/3501-6 carbon/epoxy with a $[45/0/-45/90]_{6S}$ layup. See figure 18. The impacter had a diameter of 12.7 mm. The mechanical properties of IM7/8551-7 and AS4/3501-6 are very similar, and the results should be applicable to either.

Contact force is plotted against time in figure 19 for impacter velocities of 7.73, 16.5, and 52.1 m/s. For a given value of kinetic energy, impacter mass

varies inversely with impacter velocity squared. Thus, increasing velocity is equivalent to decreasing mass. The duration of the impacts increase with decreasing velocity (increasing mass). For velocities of 7.73 and 16.5 m/s, the contact force history consists of small amplitude plate vibrations superimposed on the forced response associated with momentum exchange. For the 52.1 m/s velocity, the forced response is too short for the vibrations to be apparent.

The values of contact force for the first peak of the force-time history, the second peak, the third peak, and so forth are plotted against impacter velocity in figure 20 as solid and dashed lines for a kinetic energy of 13.6 J. The upper envelope or maximum values of the peaks are represented by the solid line. The maximum contact force will be referred to as the impact force. For this reason, the relationship between impact force (or any other measure of plate response) and impacter velocity (or mass) will not be smooth but will contain cusps because of the vibratory response of the plate. On the whole, impact force in figure 20 increases with increasing velocity (and decreasing mass). The velocities are divided into two regions: falling weight and pendulum (1-10 m/s) and ballistic tests (10-200 m/s). For velocities below 10 m/s, impact force is relatively constant as indicated by equation (1); but, for velocities greater than 10 m/s, impact force increases significantly with velocity. Results are not shown for velocities below 1 m/s because of convergence problems in making calculations. It is expected that the impact force curve (solid curve) would approach an asymptote not too much below that for the lowest velocity shown.

The impact force is also plotted against impacter velocity in figure 20 for a kinetic energy of 20.3 J. For low velocities, the impact force for 20.3 J is approximately 1.23 times that for 13.6 J. From equation (1), the impact force for 20.3 J is 1.22 to 1.27 times that for 13.6 J, $(20.3/13.6)^{0.5}$ to $(20.3/13.6)^{0.6}$. Thus, equation (1) and the impact analysis are in agreement for small velocities. Moreover, this ratio holds approximately for the entire range of velocities.

Deflection of the plate and impacter are plotted against impacter velocity in figure 21. For low and high velocities, the impacter deflects more than the plate indicating contact. The difference is the indentation of the plate, which was represented by Hertzian contact. Between velocities of 2 and 4 m/s, the plate and impacter are not in contact, indicating multiple impacts. For velocities less than 10 m/s, the deflection of the plate and impacter are approximately independent of velocity. For velocities greater than 10 m/s, the deflection of the plate and impacter decrease dramatically with increasing velocity.

The maximum values of back-face tension strains at the center of the plate and midway between the center and edge is plotted against impacter velocity in figure 22. The x and y components of strain are equal at the center where they are also greatest. The strain at the center is a minimum at the cusp near 23 m/s. Except near this cusp, the strain at the center increases less than 20 percent with increasing velocity.

DISCUSSION

Static Indentation Versus Falling Weight Tests

For the static indentation and falling weight tests of the AS4/3501-6 and IM7/8551-7 tape materials, the sizes of damage in the C-scan maps and the residual compression strengths were in agreement for a given contact or impact force. Near the contact region, damage consisted of matrix cracking, delaminations, and broken fibers. Away from the contact region, damage consisted principally of delaminations. Thus, the size of damage measured in the C-scans are associated with delamination size. Delaminations developed at each of the -45/0 ply interfaces, making failure by sublaminate buckling probable. Residual compression strengths decreased with increasing damage size, consistent with failure by sublaminate buckling [16].

For impacter velocities less than 20 m/s, plate analysis revealed that impact force and back-face strain varied little with velocity for a given kinetic energy. Delamination size is associated with impact force. Since impacter velocities were less than 6 m/s for the static indentation and falling weight tests, the analysis confirms that damage size should have been the same for static indentation and falling weight tests for a given kinetic energy.

For the static indentation and falling weight tests, damage became visible on the front face at a lower impact force than on the back face. The threshold for visible damage and for penetration was greater for IM7/8551-7 than for AS4/3501-6. However, the impact forces at which damage became visible on the front and back faces were somewhat different for the two types of tests. On the front face, the impact force at which damage became visible was smaller for the static indentation test than for the falling weight test, more so for IM7/8551-7 than for AS4/3501-6. On the back face, damage became visible before penetration for the falling weight test, but penetration occurred before damage became visible for the static indentation test.

Falling Weight Versus Ballistic Tests

For AS4/3501-6, the damage sizes for a given kinetic energy were somewhat larger for the falling weight tests than for the ballistic tests, and the compression strengths were equal except for the lowest energies where the strengths were somewhat less for the falling weight tests than the ballistic tests. For IM7/8551-7, the damage sizes and compression strengths were equal for the two types of tests. Apparently, the high interlaminar toughness ameliorated differences between the falling weight and ballistic tests. For a given kinetic energy, damage sizes for IM7/8551-7 were less than half those for AS4/3501-6, and the energy threshold for causing damage was less for AS4/3501-6 than for IM7/8551-7. Thus, the IM7/8551-7 was more resistant to matrix damage than AS4/3501-6, which is consistent with the greater interlaminar toughness of IM7/8551-7.

Opposite to the AS4/3501-6 and IM7/8551-7 tape materials, damage sizes for the braided material were significantly smaller and compression strengths were larger for the falling weight tests than for the ballistic tests. Near the contact site, damage consisted of broken fibers, matrix cracks, and disbonded

yarns. Away from the contact site, damage consisted primarily of disbonded yarns. Thus, damage size in the radiographs is associated with disbonded yarns. Strengths varied inversely with damage size as they did with the tape materials.

One possible cause for the opposite response of the tape and braided materials is the difference between boundary conditions during impact. The plates were clamped for the tape materials and simply supported for the braided material. To determine the significance of boundary conditions, impact force is plotted against impacter velocity in figure 23 for simply supported and clamped plates. Recall that impacter velocities were between 1 and 6 m/s for the falling weight tests and between 41 and 160 m/s for the ballistic tests. The plates were assumed to be 12.7- by 12.7-mm and made of AS4/3501-6 carbon/epoxy with a $[45/0/-45/90]_{6S}$ layup. The impacter diameter was 12.7 mm, and the kinetic energy is constant, 13.6 J. The simply supported curve was taken from figure 20. The equations in [9] and [15] can only be used to analyze the impact of a simply supported plate. The response of the clamped plate was estimated using that of the simply supported plate. At the lowest velocity, the impact force was assumed to increase in proportion to the square root of plate stiffness (equation (1) with relatively large n_0). The ratio of displacements for the clamped and simply supported plates was calculated for static loading. The impact force for the simply supported plate at the lowest velocity was then multiplied by the square root of that ratio. The curve for the simply supported plate was then rotated upward about the right-hand end because boundary conditions do not affect impact force for large velocities (small masses) [7]. The overall effect of clamping the plate is to reduce or eliminate the increase in impact force with increasing impacter velocity. In other words, the differences between impact force for low and high velocities should be less for a clamped plate than for a simply supported plate. The effect of simply supported and clamped boundaries on back-face strain should be similar to that on impact force.

Since damage size is expected to increase with increasing impact force, the results in figure 23 indicate that damage size should increase with increasing velocity for simply supported plates but not necessarily for clamped plates. Thus, the curves in figure 23 are consistent with the experiments. That is, for the simply supported plates made of the braided material, damage size should be greater for the ballistic tests than for the falling weight tests but not necessarily for the clamped plates made of the tape materials.

Another contribution to the opposite response of the tape and braided materials is the difference between impacter materials. For the braided material, the impacters for the pendulum and ballistic tests were made of steel. For the AS4/3501-6 and IM7/8551-7 tape materials, the impacter for the falling weight tests was also made of steel, whereas the impacter for the ballistic tests was an aluminum sphere. For the highest velocities, the aluminum spheres flattened significantly, indicating that the aluminum yielded. Thus, some of the kinetic energy was converted to nonreversible strain energy when the aluminum yielded, perhaps as much as 1 to 10 J. This absorbed energy would have the effect of reducing the kinetic energy of the impacter. If the highest values of kinetic energy for the ballistic tests in figures 5(a), 5(b), 10(a), and 10(b) are reduced by 10 J, the ballistic tests are as severe as the falling weight tests for AS4/3501-6 and more severe than the falling weight tests for IM7/8551-7.

For the AS4/3501-6 and IM7/8551-7 tape materials, the states of internal damage were similar for a given type of test but somewhat different for the falling weight and ballistic tests. For the falling weight tests, the damage extended uniformly from the contact surface to the back face; whereas, for the ballistic tests, the damage was mostly absent in a small zone from the contact surface to the midplane.

Damage tolerance actually has two distinct facets: the resistance to damage and the tolerance to damage. The resistance to damage is measured by the extent or size of damage for a given impact energy or impact force; whereas, the tolerance to damage is measured by the strength loss for a given size of damage. Of the three materials tested, the resistance to damage was greatest for the IM7/8551-7 tape material and least for the braided material. Compare figures 5(a), 5(b), and 8. On the other hand, damage tolerance was greatest for the braided material and least for the AS4/3501-6 and IM7/8551-7 tape materials. Compare figures 12(a), 12(b), and 13. The damage tolerance of the IM7/8551-7 and AS4/3501-6 tape materials was nearly equal, indicating that both materials probably fail by sublaminate buckling. The failure mode of the braided material was obviously not sublaminate buckling because the disbonded yarns did not form large planes of delamination. Probably failure was precipitated by buckling of the disbonded yarns.

Analysis of the falling weight and ballistic test results in terms of impact force would have been of great assistance in understanding the impact response. The original intent of measuring contact diameters for the tape laminates was to estimate impact forces for the ballistic tests. The impact force [5] is given by

$$F_{max} = r_c^3 \, n_0 / R_i \tag{10}$$

where r_c is the contact radius, R_i is the radius of the spherical impacter and n_0 is the Hertzian spring constant in equation (1). Thus, for a given material and impacter radius, impact force is uniquely related to contact radius. Instead of equation (10), the actual contact diameter versus impact force data for the static indentation and falling weight tests were going to be used for a calibration curve. For the static indentation and falling weight tests, contact diameters were in good agreement with one another for a given impact force. The contact diameters for AS4/3501-6 and IM7/8551-7 were also in good agreement except near penetration. See figure 16. However, the contact diameters for the ballistic tests were 1.2 to 1.4 times those for the falling weight tests for a given kinetic energy. See figure 17. Because the impact force is proportional to contact radius to the third power, the contact diameters indicate that impact forces for the ballistic tests were 1.8 to 2.8 times those for the falling weight tests, which is inconsistent with the smaller damage sizes and larger residual compression strengths for the ballistic tests. Thus, the plan for calculating impact forces for the ballistic tests using contact diameters was abandoned.

The carbon and white papers were not bonded to the composite. Possibly, the papers, which were highly accelerated in the ballistic tests, wrapped around the sphere and inflated the contact diameters. The sensitivity of impact force to variations in contact diameter may render calculations of impact force by

this method qualitative at best. Thus, efforts should be made to develop some other method to measure ballistic impact forces.

Also, the curves in figure 23 indicate that boundary conditions for static indentation and falling weight tests (low velocities) significantly affect impact force for a given kinetic energy. However, it is expected that impact response would be essentially the same for simply supported and clamped boundaries for a given impact force.

CONCLUDING REMARKS

Static indentation, falling weight, and ballistic tests were conducted on laminates made of AS4/3501-6 and IM7/8551-7 prepreg tape. The $[45/0/-45/90]_{6S}$ laminates were 7 mm thick. Pendulum and ballistic tests were also conducted on a 20^{0} braided material made of Celion 12000 fibers and 3501-6 epoxy, which was about 5-mm thick. The AS4/3501-6 and IM7/8551-7 plates were clamped and the braided plates were simply supported on all sides during impact. The impacters had spherical or hemispherical shapes with a 12.7 mm diameter. Kinetic energies ranged from 5-50 J. Masses for the falling weight and pendulum tests were 4.63 and 13.84 kg, respectively, and velocities ranged from 1-5 m/s. Masses for the ballistic tests were 3.0 and 14.5 g and the velocities ranged from 40-160 m/s. Residual compression strengths, back-face strains, and damage sizes were measured for the static indentation, falling weight, and pendulum tests. Impact forces were measured for all but the ballistic tests. Contact areas were measured for all tests of the AS4/3501-6 and IM7/8551-7 material. An impact analysis was conducted using plate equations to aid in understanding the experimental results.

No significant differences were noticed between the static indentation and falling weight tests of AS4/3501-6 and IM7/8551-7. Sizes of damage and residual compression strengths were in agreement for a given contact or impact force. Damage size was associated principally with delamination size. The impact analysis confirmed that damage size should be relatively independent of velocity for velocities less than 20 m/s for a given kinetic energy.

Also, no significant differences were noticed between the falling weight and ballistic tests of AS4/3501-6 and IM7/8551-7. Residual compression strengths were in agreement for a given kinetic energy. Sizes of damage for IM7/8551-7 were in agreement, but sizes of damage for AS4/3501-6 were a little larger for the falling weight tests than the ballistic tests. Some of this difference can be attributed to inelastic deformation of the aluminum spheres that were used in these ballistic tests. The impact analysis also indicated that, for clamped boundaries, damage size may be relatively independent of velocity for velocities between 20 and 160 m/s for a given kinetic energy. For static indentation, falling weight, and ballistic tests, strengths varied inversely with damage size consistent with failure by sublaminate buckling.

On the other hand, significant differences were noticed between the pendulum and ballistic tests of the braided material. Sizes of damage were significantly less and compression strengths were significantly more for the falling weight tests than for the ballistic tests. Strengths varied inversely

with damage size. The impact analysis also indicated that, for simply supported boundaries, damage size should increase significantly with increasing velocity for velocities between 20 and 160 m/s for a given kinetic energy. Thus, ballistic tests are more severe than falling weight tests when plates are simply supported but not necessarily when plates are clamped.

Of the three materials tested, the sizes of damage were least for the IM7/8551-7 tape material and greatest for the braided material for a given kinetic energy. On the other hand, the strength loss as a fraction of original strength was least for the braided material and greatest for the AS4/3501-6 and IM7/8551-7 tape materials for a given size of damage. The strength loss for the IM7/8551-7 and AS4/3501-6 tape materials was nearly equal, which is consistent with both tape materials failing by sublaminate buckling. The failure mode of the braided material was obviously not sublaminate buckling because the disbonded yarns do not form large planes of delamination. Failure was probably precipitated by buckling of the disbonded yarns.

REFERENCES

1. Rhodes, Marvin D.: Impact Tests on Fibrous Composite Sandwich Structures. NASA TM 78719, October 1978.

2. Williams, Jerry G.: Comparison of Toughened Composite Laminates using NASA Standard Damage Tolerance Tests. NASA CP 2321, August 1984.

3. Williams, Jerry G.: Effect of Impact Damage and Open Holes on the Compression Strength of Tough Resin/High Strain Fiber Laminates. NASA TM 85756, February 1984.

4. Portanova, M. A.; Poe, Jr. C. C.; and Whitcomb, John D.: Open Hole and Post-Impact Compression Fatigue of Stitched and Unstitched Carbon/Epoxy Composites. NASA TM 102676, June 1990.

5. Poe, Jr. C. C.: Summary of a Study to Determine Low-Velocity Impact Damage and Residual Tension Strength for a Thick Graphite/Epoxy Motor Case. NASA TM 102678, June 1990.

6. Cantwell, W. J. and Morton J.: The Influence of Varying Projectile Mass on the Impact Response of CFRP. Composite Structures, 13, 1989, pp. 101-114.

7. Cantwell, W. J. and Morton J.: Comparison of the Low and High Velocity Impact Response of CFRP. Composites, Vol. 20, No. 6, November 1989, pp. 545-551.

8. Elber, Wolf: Failure Mechanics in Low-Velocity Impacts on Thin Composite Plates. NASA TP 2152, May 1983.

9. Sankar, Bhavani V.: A Modified Green's Function for Computing Structural Response due to Low-Velocity Impact. Department of Aerospace Engineering, Mechanics & Engineering Science, University of Florida, Gainesville, Florida 32611, Technical Report No. AeMES-TR-1-36, October 1990.

10. Johnston, N. J. and Hergenrother, P. M.: High Performance Thermoplastics: A Review of Neat Resin and Composite Properties. 32nd International SAMPE Symposium & Exhibition, Anaheim, April 6-9, 1987, Also NASA TM 89104.

11. Dow, Marvin B. and Smith, Donald L.: Properties of Two Composite Materials Made of Toughened Epoxy Resin and High Strain Graphite Fiber. NASA TP 2826, July 1988.

12. Palmer, R.; Dow, Marvin B.; and Smith, Donald L.: Development of Stitching Reinforcement for Transport Wing Panels. First NASA Advanced Composites Technology (ACT) Conference, NASA CP-3104, Part 2, 1991, pp. 621-646.

13. Simonds, Robert A.; Stinchcomb, Wayne; and Jones, Robert M.: Mechanical Behavior of Braided Composite Materials. Composite Materials: Testing and Design (Eighth Conference), ASTM STP 972, J. D. Whitcomb, Ed., American Society for Testing and Materials, Philadelphia, 1988, pp. 438-453.

14. SACMA SRM 2-88 (Suppliers of Advanced Composite Materials Association): Recommended Test Method for Compression after Impact Properties of Oriented Fiber-Resin Composites.

15. Sankar, B. V.; Ku, C.; and Nguyen, P. T.: Nondimensional Impact Models for Composite Laminates. Fifth Technical Conference of the American Society for Composites, June, 1990.

16. Ilcewicz, Larry B.; Dost, Ernest F.; and Coggeshall, Randy L.: A Model for Compression after Impact Strength Evaluation. 21st International SAMPE Technical Conference, Volume 21, Advanced Materials: The Big Payoff, Atlantic City, N.J. Sept. 25-28, 1989, pp, 130-140.

TABLE I.- Impact test data for [45/0/-45/90]6S AS4/3501-6 tape laminate.

Test no.	Kinetic energy, J	Mass, g	Velocity, m/s	Impact force, kN	Damage size in C-scan, cm^2	Contact dia., mm	Compression strength, MPa	Front face damage (a)	Back face damage (a)
ST11A	-	-	0	2.33	0	2.8	530.	NV	NV
ST13A	-	-	0	7.12	0	4.1	527.	NV	NV
ST04A	-	-	0	7.52	2.84	4.3	531.	NV	NV
ST03A	-	-	0	8.14	11.3	5.0	223.	NV	NV
ST01A	-	-	0	9.05	12.5	5.2	209.	D	NV
ST14A	-	-	0	10.3	14.7	5.4	209.	D	NV
ST12A	-	-	0	13.3	26.7	6.0	176.	D	NV
ST02A	-	-	0	15.2	87.1	-	97.9	P	P
D01A	6.78	4630	1.71	6.45	8.06	4.7	260.	NV	NV
D02A	13.6		2.42	10.0	11.3	5.1	186.	D	NV
D03A	20.3		2.97	11.6	24.6	5.4	171.	D	B,MC
D04A	27.1		3.43	12.0	22.7	5.6	166.	D,BF	B,MC
D05A	27.1		3.43	-	18.4	5.6	(b)	D,BF	B,MC
D06A	37.7		4.04	13.3	33.5	7.7	144.	D,BF	B,BF
D07A	47.5		4.53	13.8	22.1	9.0	131.	D,BF	B,BF
D08A	61.0		5.14	-	35.5	11.6	128.	D,BF	B,BF
D11A	6.78	3.00	67.8	-	3.16	5.5	485.	NV	NV
D12A	13.6		95.3	-	10.0	6.1	202.	D	NV
D17A	13.6		96.0	-	13.7	6.4	220.	NV	NV
D13A	20.3		114.	-	9.74	6.7	175.	D	NV
D14A	27.1		135.	-	12.2	7.0	153.	BF	NV
D15A	27.1		135.	-	13.9	7.5	(c)	BF	MC
D16A	37.7		160.	-	21.4	7.2	126.	BF	BF

a - Code for damage on surface.
NV - No damage was visible.
D - Dent.
P - Penetration.
B - Bump or protuberance.
MC - Matrix crack.
BF - Broken fibers.

b - Specimen was sectioned and deplied. Fibers were broken in first 9 plies of the outer face.

c - Specimen was sectioned and deplied. No fibers were broken.

TABLE II.- Impact test data for [45/0/-45/90]6S IM7/8551-7 tape laminate.

Test no.	Kinetic energy, J	Mass, g	Velocity, m/s	Impact force, kN	Damage size in C-scan, cm^2	Contact dia., mm	Compression strength, MPa	Front face damage (a)	Back face damage (a)
ST06IR	-	-	0	2.22	0	3.0	489.	NV	NV
ST13IP	-	-	0	3.18	0	3.3	500.	NV	NV
ST03IR	-	-	0	4.49	0	3.9	481.	NV	NV
ST12IP	-	-	0	5.81	0	3.9	517.	NV	NV
ST07IR	-	-	0	7.16	0	4.3	448.	NV	NV
ST01IR	-	-	0	8.86	.19	4.8	498.	D	NV
ST04IR	-	-	0	10.6	.26	5.3	465.	D	NV
ST02IR	-	-	0	13.3	4.06	5.7	332.	D	NV
ST11IP	-	-	0	15.9	8.97	6.1	309.	D	NV
ST05IR	-	-	0	19.9	45.0	-	164.	P	P
D01IR	6.78	4630	1.71	8.98	0	4.7	510.	NV	NV
D02IR	13.6		2.42	10.2	3.48	5.4	380.	NV	NV
D03IR	20.3		2.97	12.7	4.58	-	364.	NV	NV
D04IR	27.1		3.43	14.5	6.64	5.7	321.	D	NV
D05IR	27.1		3.43	14.7	5.68	5.6	(b)	D	NV
D11IP	37.7		4.04	17.1	8.77	6.0	270.	D,BF	D,BF
D12IP	47.5		4.53	18.3	11.2	8.2	228.	D,BF	B,BF
D13IP	54.2		4.84	18.7	12.8	9.0	225.	D,BF	B,BF
D14IP	61.0		5.14	18.7	14.1	9.0	216.	D,BF	B,BF
D07IR	6.78	3.00	68.4	-	0	6.0	493.	NV	NV
D19IP	6.78		66.0	-	0	5.5	479.	NV	NV
D18IP	13.6		94.5	-	2.84	6.6	439.	D	NV
D08IR	13.6		95.2	-	2.97	6.7	433.	D	NV
D09IR	20.3		117.	-	4.77	7.8	341.	D	NV
D16IP	27.1		135.	-	5.61	7.5	297.	D	NV
D10IR	27.1		134.	-	5.81	8.2	312.	D	NV
D17IP	37.7		159.	-	8.97	7.6	251.	D,BF	MC

a - Code for damage on surface.
NV - No damage was visible.
D - Dent.
P - Penetration.
B - Bump or protuberance.
MC - Matrix crack.
BF - Broken fibers.

b - Specimen was sectioned and deplied. Fibers were broken in first 3 plies of the outer face.

TABLE III.- Impact test data for CE12000/3501-6 20° braided material.

Test no.	Kinetic energy, J	Mass, g	Velocity, m/s	Impact force, kN	Damage size in radio-graph, cm^2	Compression strength, MPa
B42	14.0	13840	1.42	7.8	1.5	138.5
B46	23.7		1.85	8.7	4.9	144.1
B44	34.2		2.22	8.2	10.3	131.2
B43	49.9		2.68	8.6	20.6	113.4
B36	13.5	14.5	43.2	-	11.0	146.8
B35	30.6		65.0	-	33.5	116.5
B31	54.0		86.3	-	63.2	70.5

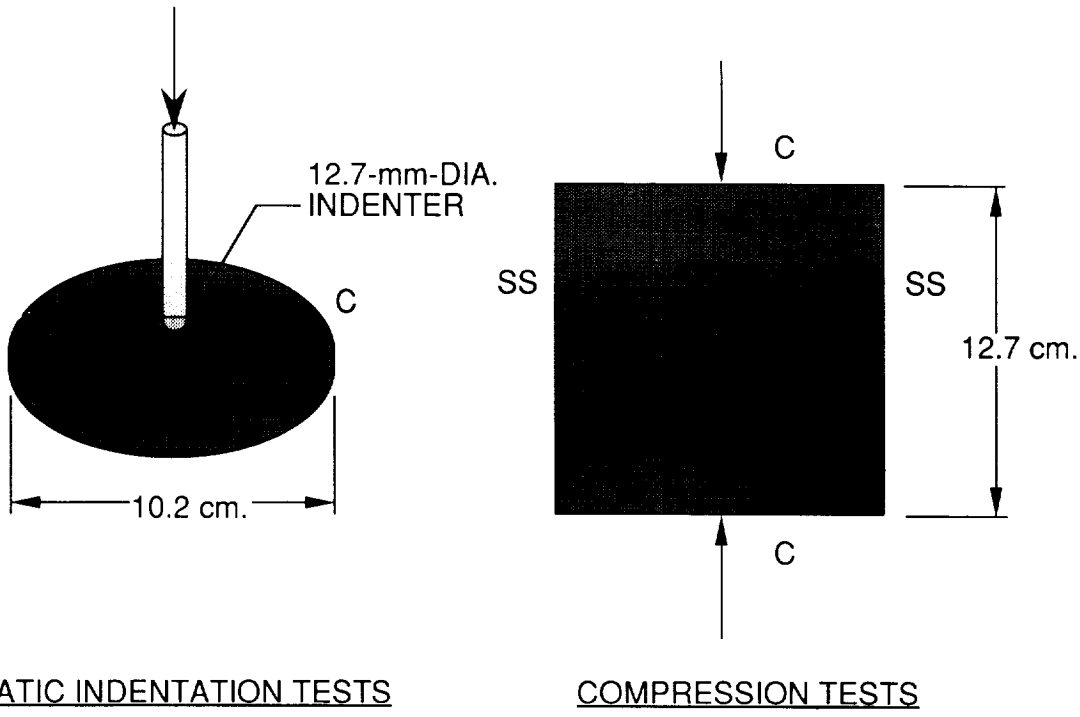

Figure 1. - Static indentation and compression tests.

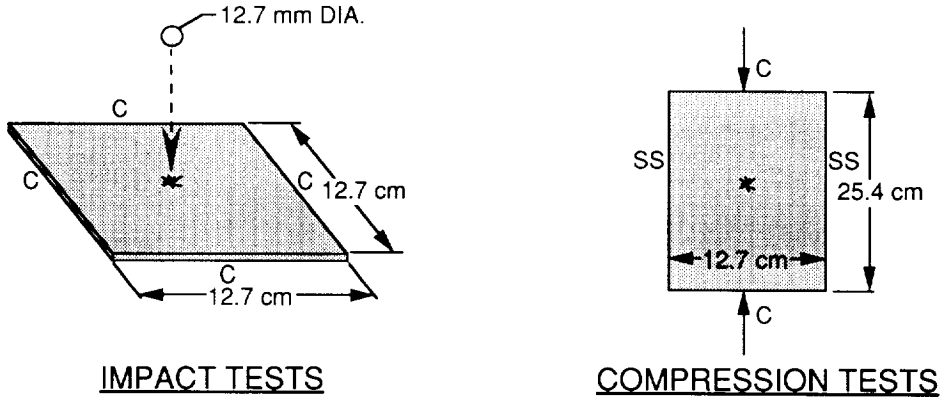

	FALLING WT.	BALLISTIC	INDUSTRY STD.
MASS	4.63 kg	0.003 kg	4.54 kg
v_1	2 - 5 m/s	68 - 160 m/s	4.54 m/s
KE	7 - 61 J	7 - 38 J	* 46.7 J

SS -- SIMPLY SUPPORTED
C -- CLAMPED

* 1500 $\frac{\text{in lbs}}{\text{in}}$

Figure 2. - Specimens and impact parameters for $[45/0/-45/90]_{6s}$ AS4/3501-6 and IM7/8551-7 tape laminates

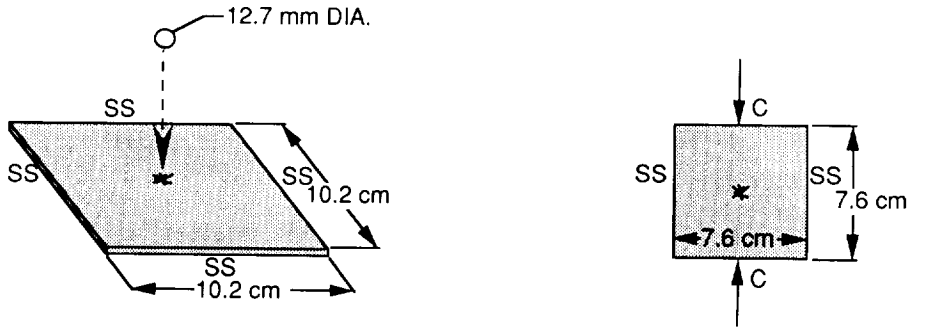

IMPACT TESTS

COMPRESSION TESTS

	PENDULUM	BALLISTIC	INDUSTRY STD.
MASS	13.84 kg	0.0145 kg	4.54 kg
v_1	1 - 3 m/s	43 - 86 m/s	3.95 m/s
KE	14 - 50 J	13 - 54 J	* 35.4 J

* 1500 $\frac{\text{in lbs}}{\text{in}}$

SS -- SIMPLY SUPPORTED
C -- CLAMPED

Figure 3. - Specimens and impact parameters for CE12000 3501-6 20° Braided material.

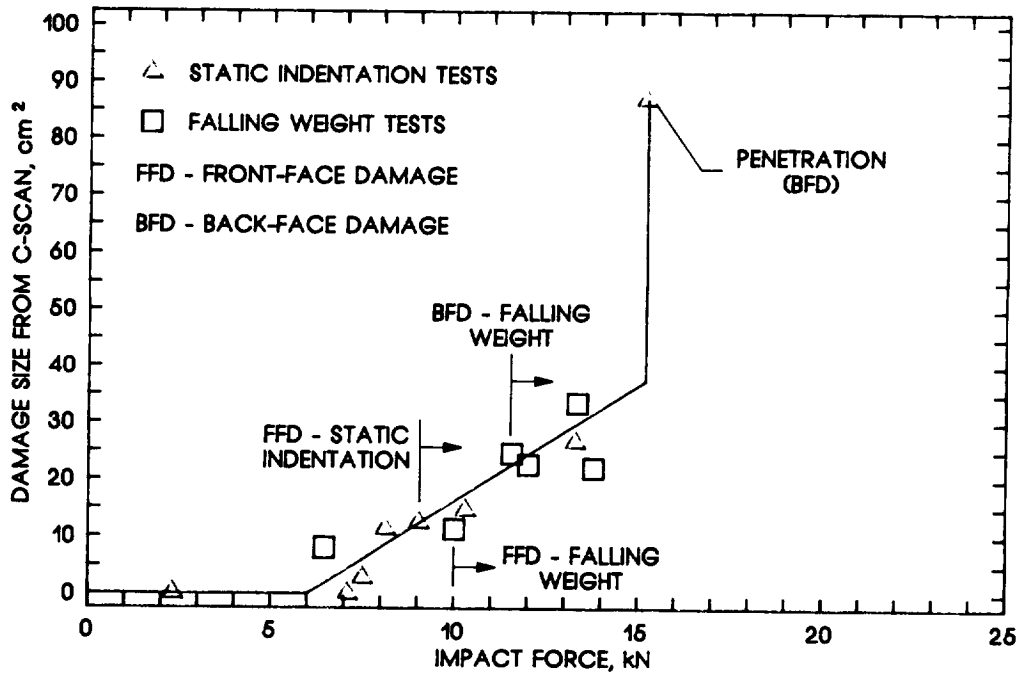

(a) $[45/0/-45/90]_{6s}$ AS4/3501-6 laminate.

Figure 4.- Damage area versus impact force.

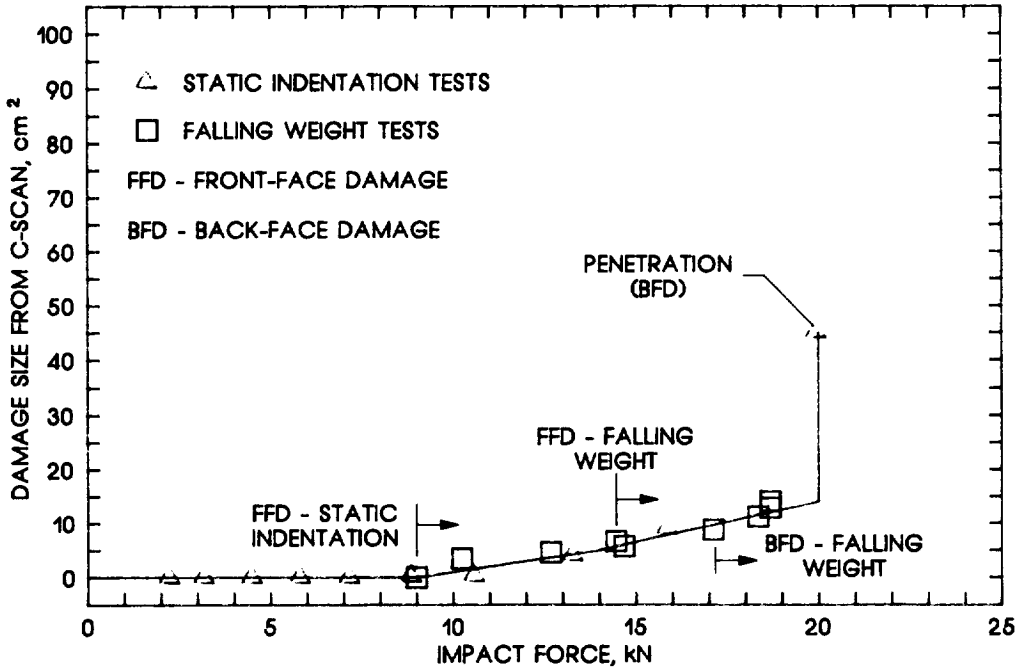

(b) $[45/0/-45/90]_{6S}$ IM7/8551-7 laminate.

Figure 4.- Concluded.

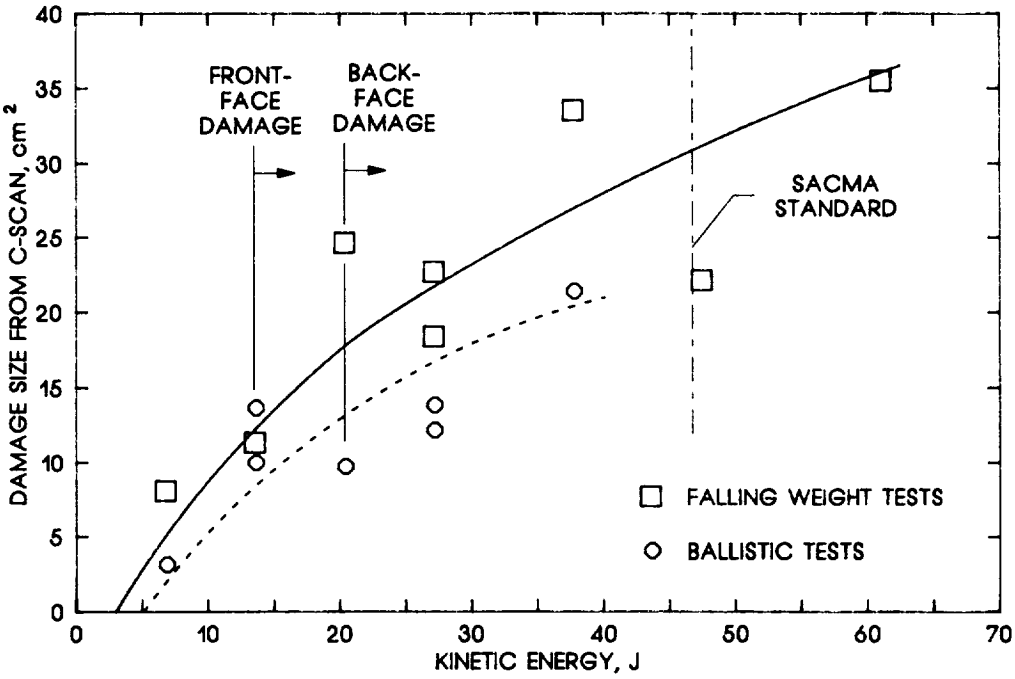

(a) $[45/0/-45/90]_{6S}$ AS4/3501-6 laminate.

Figure 5.- Damage area versus kinetic energy.

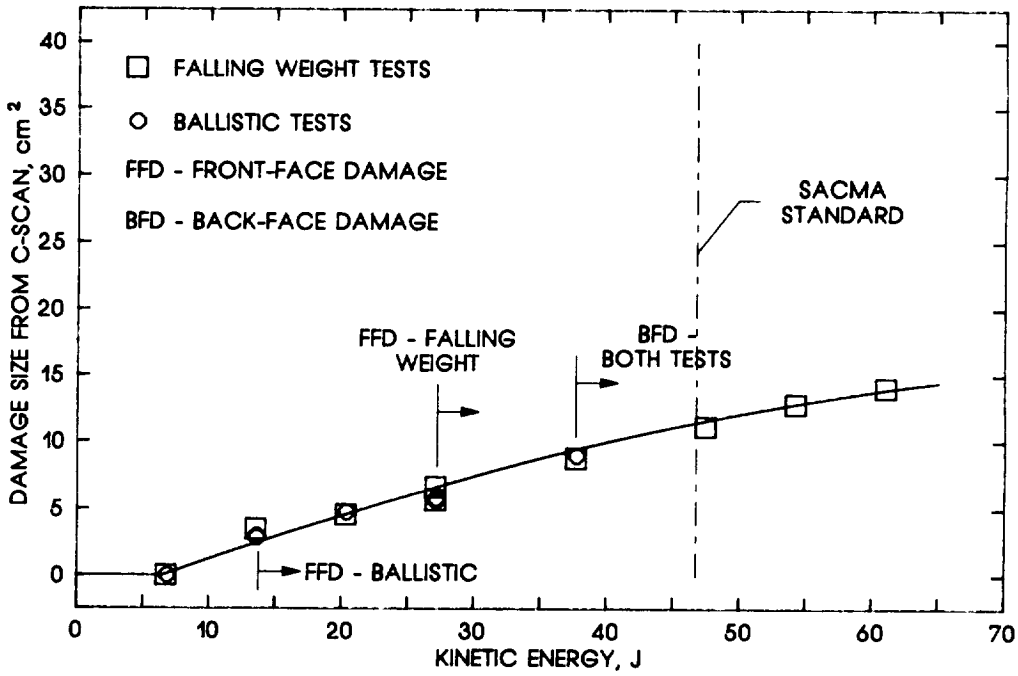

(b) $[45/0/-45/90]_{6s}$ IM7/8551-7 laminate.

Figure 5.- Concluded.

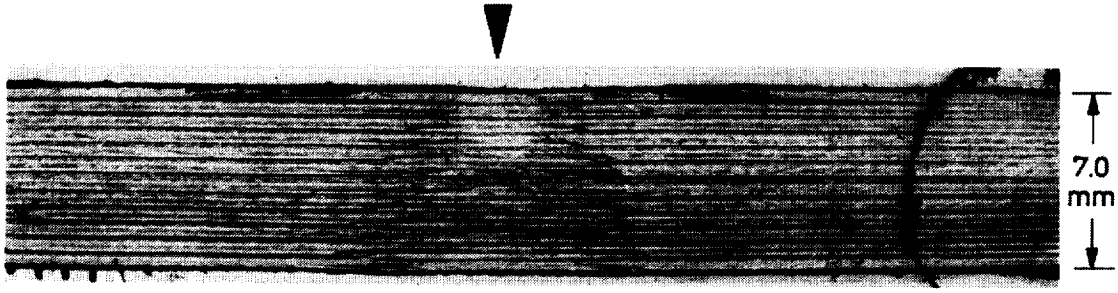

(b) Ballistic test (D15A).

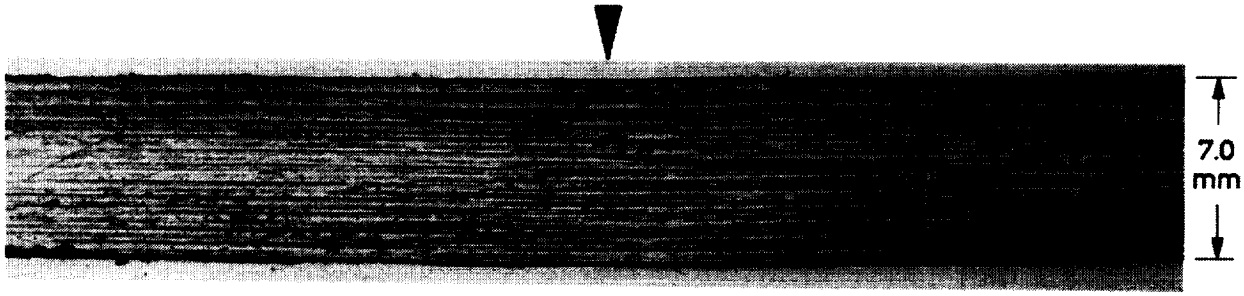

(a) Falling weight test (D05A).

Figure 6.- Photographs of edge replicas of AS4/3501-6 tape laminate impacted with kinetic energy of 27.1 J.

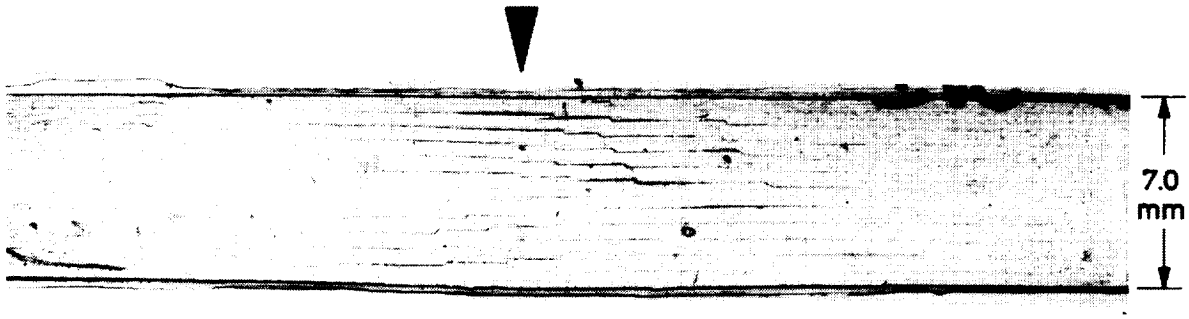

Figure 7.- Photograph of edge replica of IM7/8551-7 specimen (D05IR) impacted by falling weight with kinetic energy of 27.1 J.

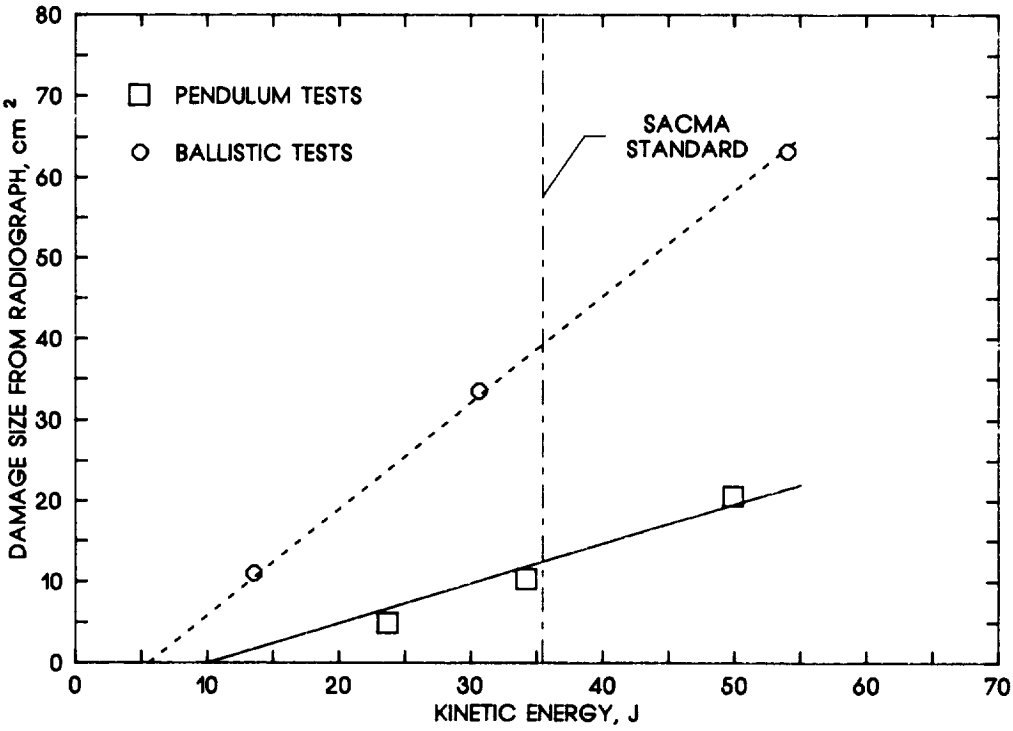

Figure 8.- Damage area versus kinetic energy for CE12000/3501-6 braided material.

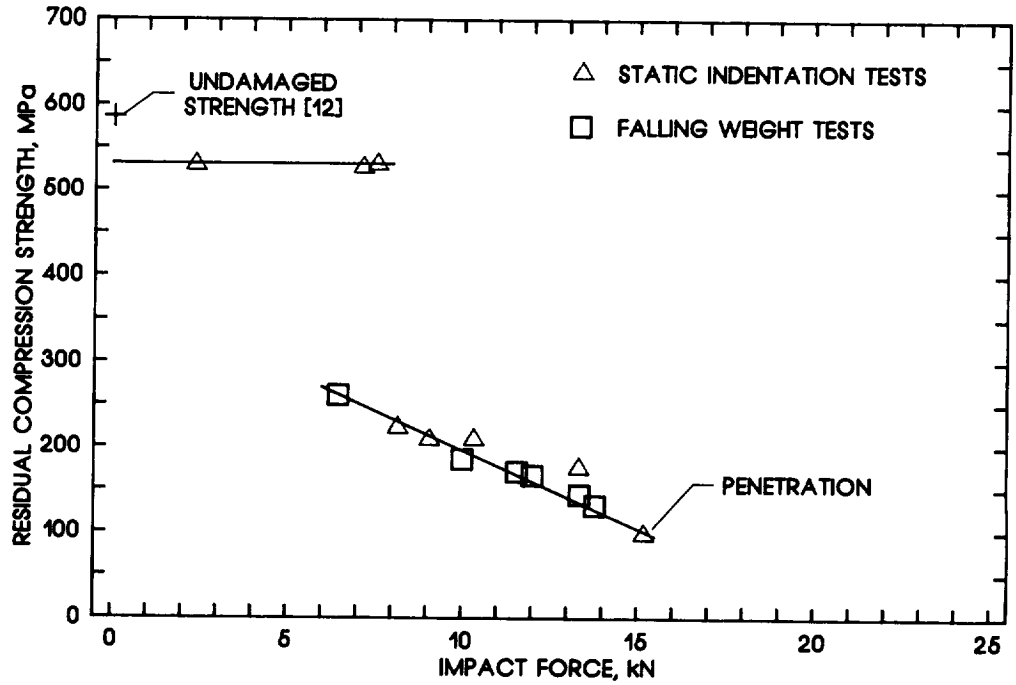

(a) $[45/0/-45/90]_{6S}$ AS4/3501-6 laminate.

Figure 9.- Residual compression strength versus impact force.

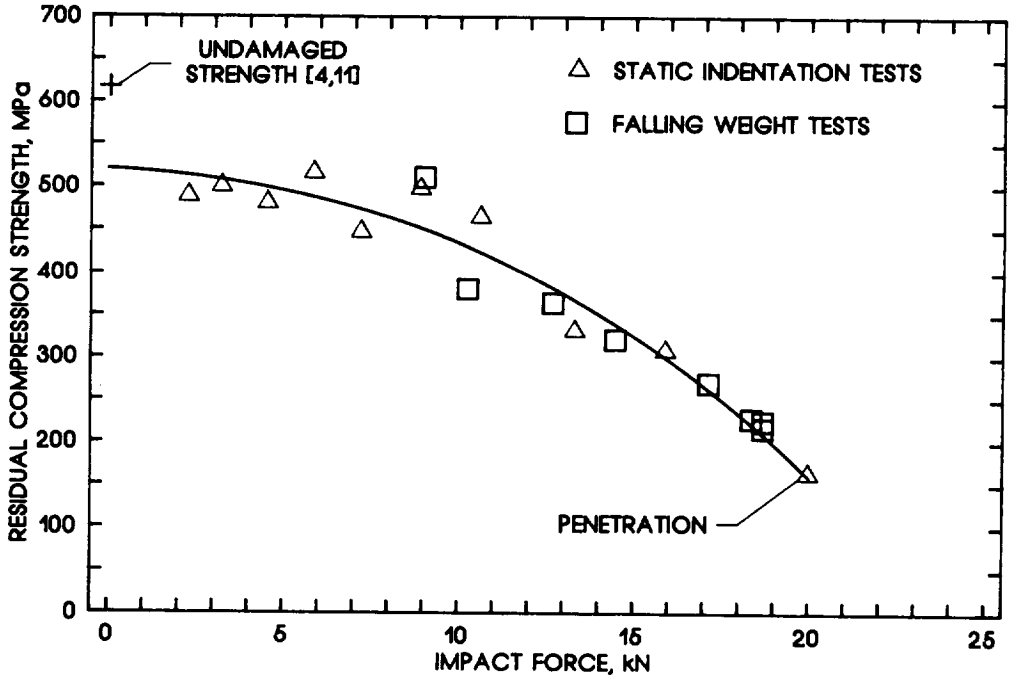

(b) $[45/0/-45/90]_{6S}$ IM7/8551-7 laminate.

Figure 9.- Concluded.

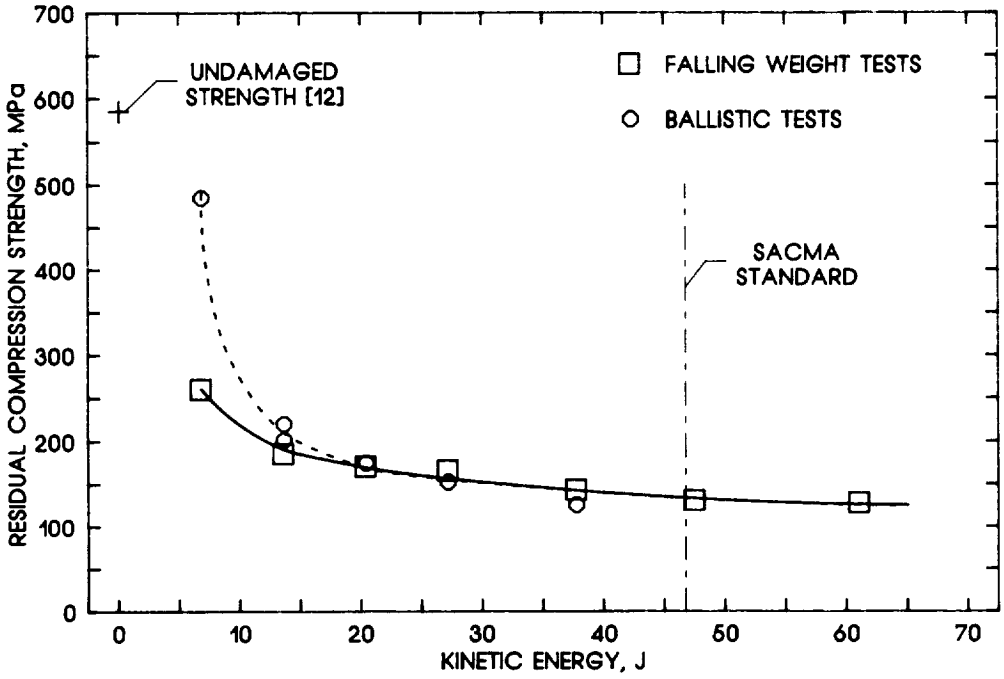

(a) $[45/0/-45/90]_{6s}$ AS4/3501-6 laminate.

Figure 10.- Residual compression strength verses kinetic energy.

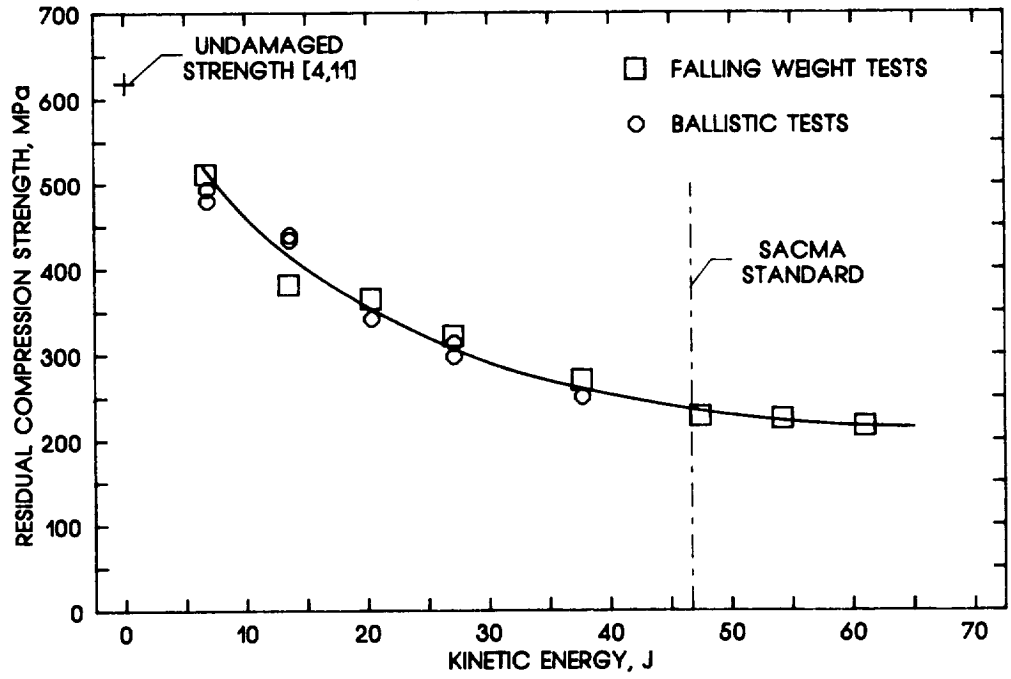

(b) $[45/0/-45/90]_{6s}$ IM7/8551-7 laminate.

Figure 10.- Concluded.

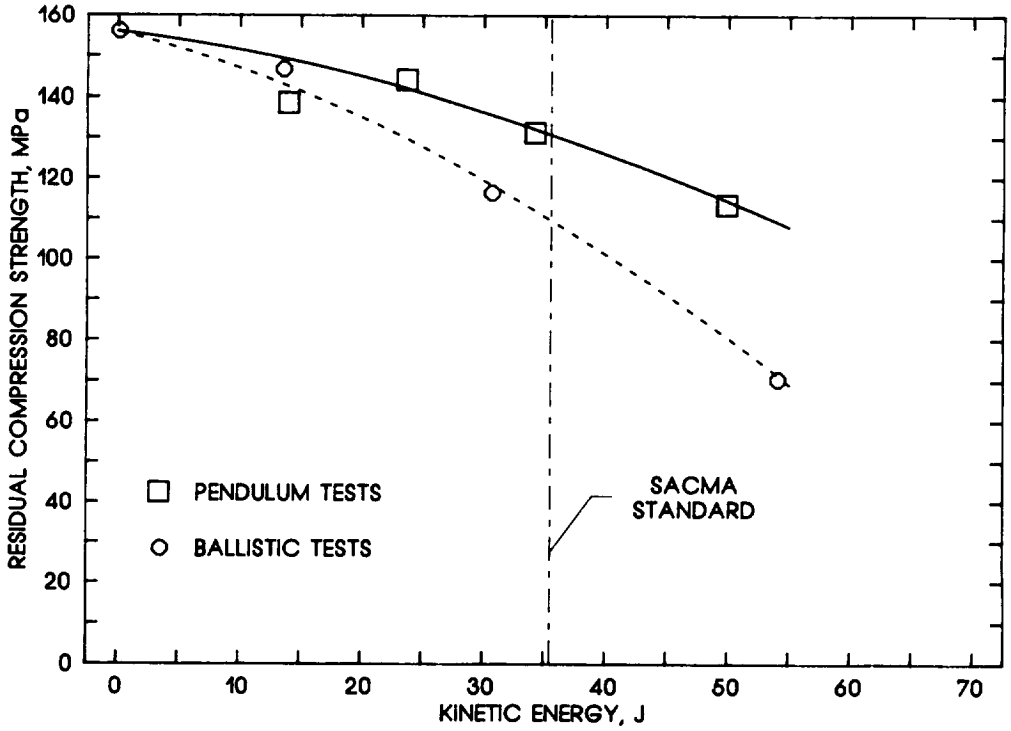

Figure 11.- Residual compression strength versus kinetic energy for CE12000/3501-6 braided material.

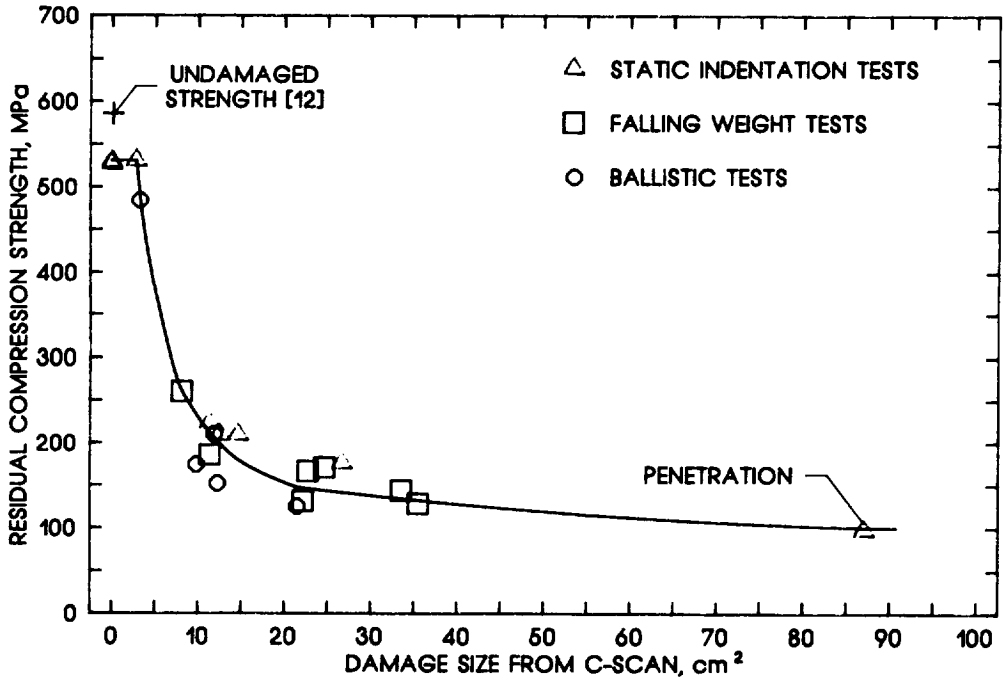

(a) $[45/0/-45/90]_{6S}$ AS4/3501-6 laminate.

Figure 12.- Residual compression strength versus damage area.

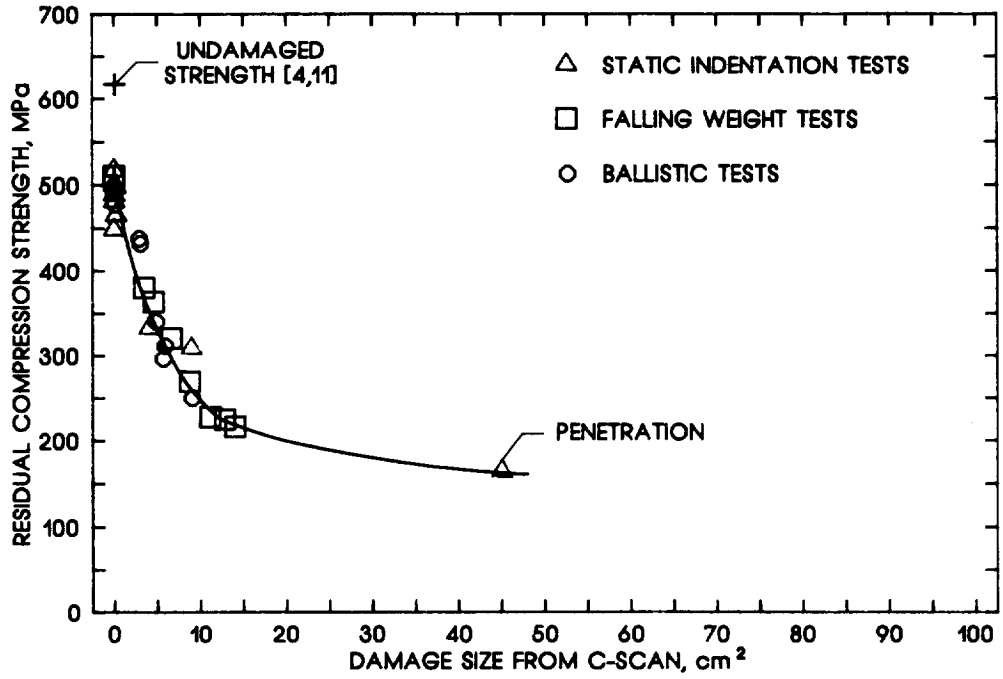

(b) $[45/0/-45/90]_{6S}$ IM7/8551-7 laminate.

Figure 12.- Concluded.

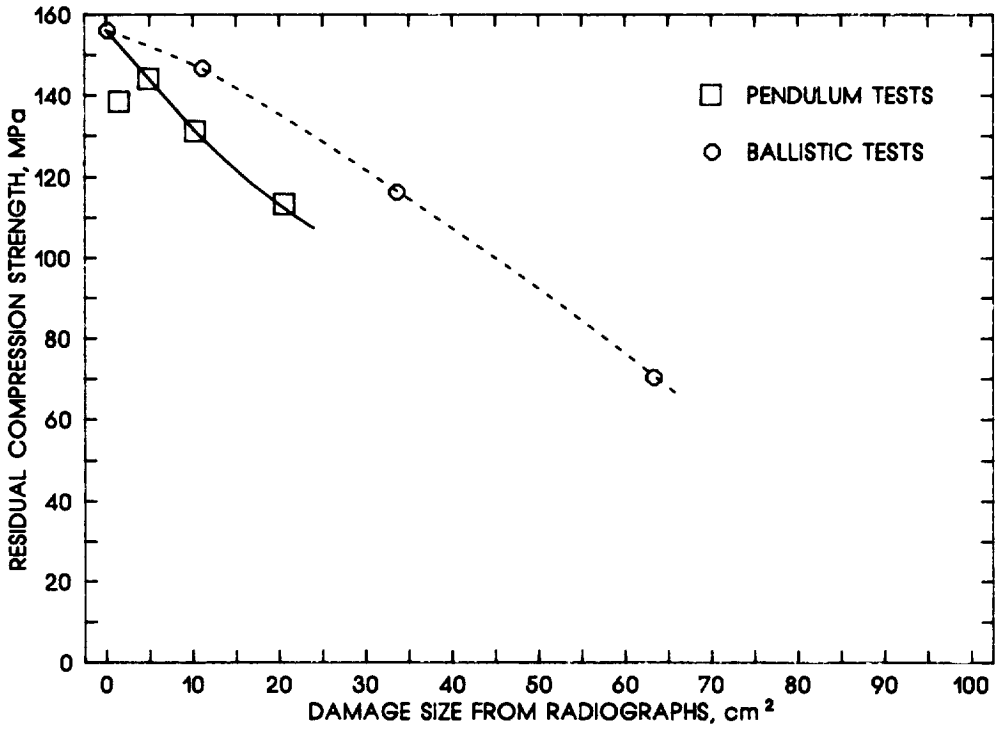

Figure 13.- Residual compression strength versus damage are for CE12000/3501-6 braided material.

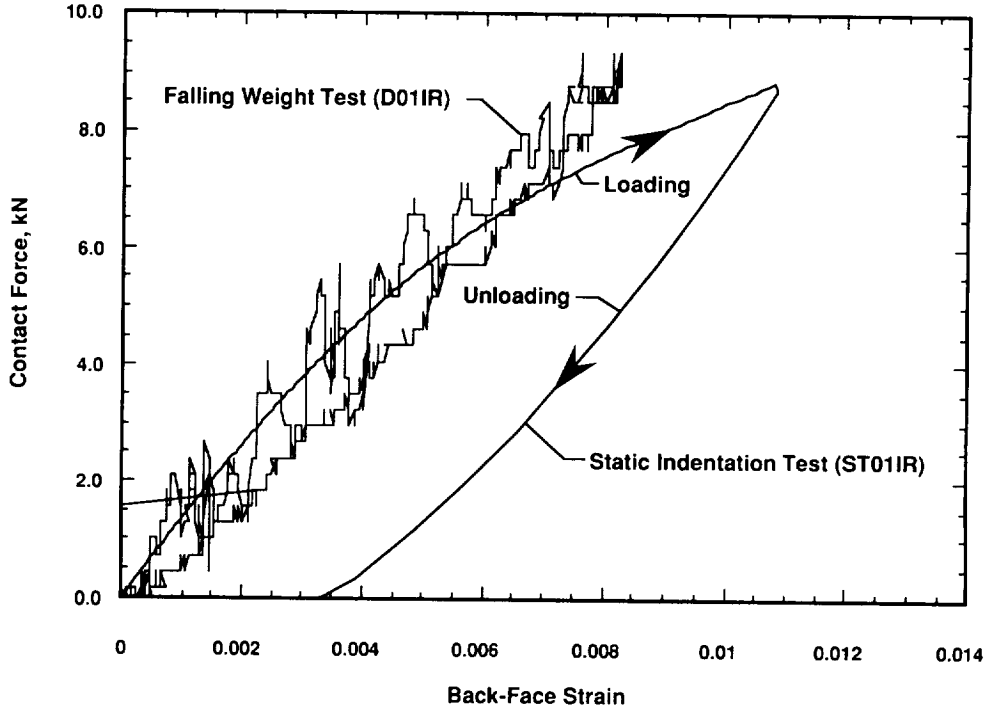

Figure 14.- Back-face strain versus contact force for static indentation and falling weight impact tests of IM7/8551-7 tape laminate

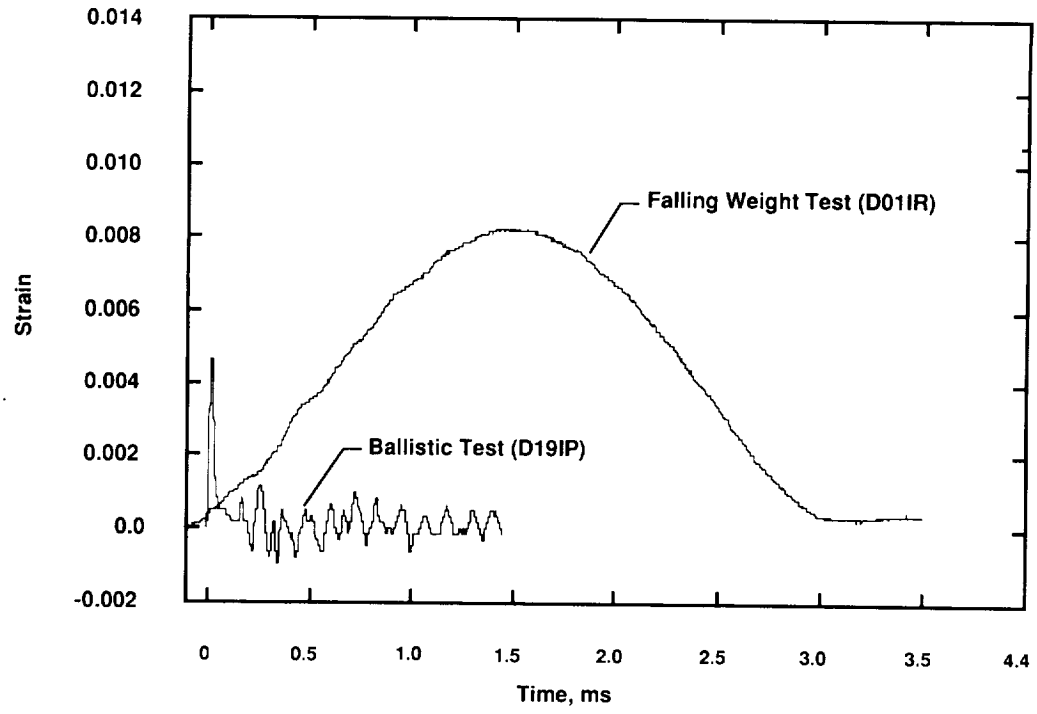

Figure 15.- Back-face strain versus time for ballistic and falling weight impact tests of IM7/8551-7 tape laminate

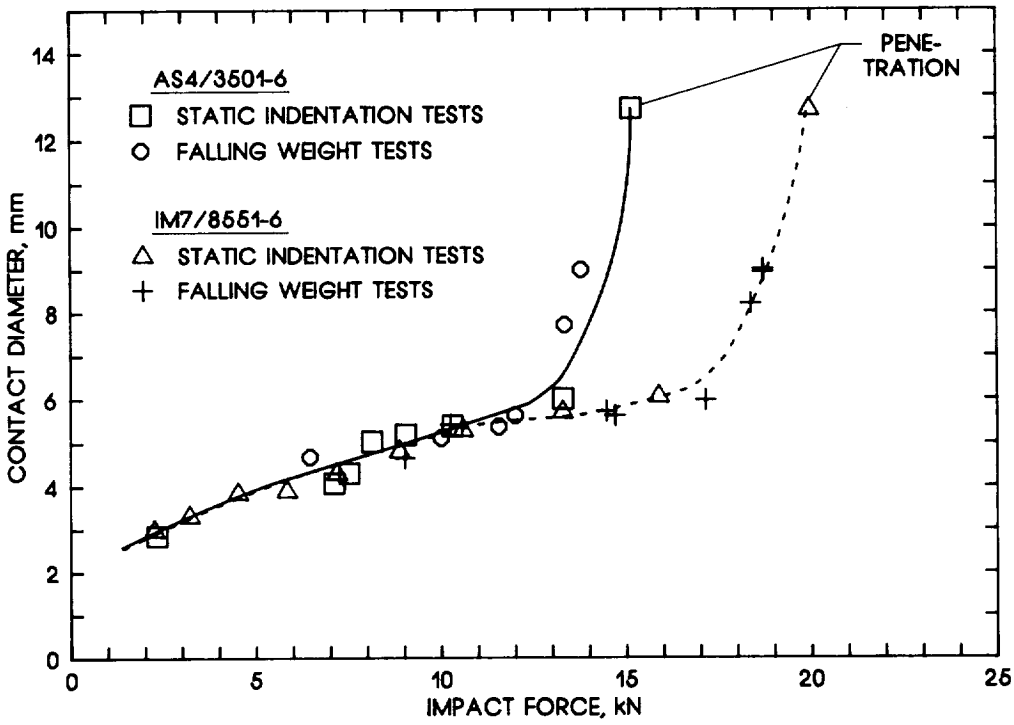

Figure 16.- Contact diameter versus impact force for $[45/0/-45/0/90]_{6s}$ tape laminates.

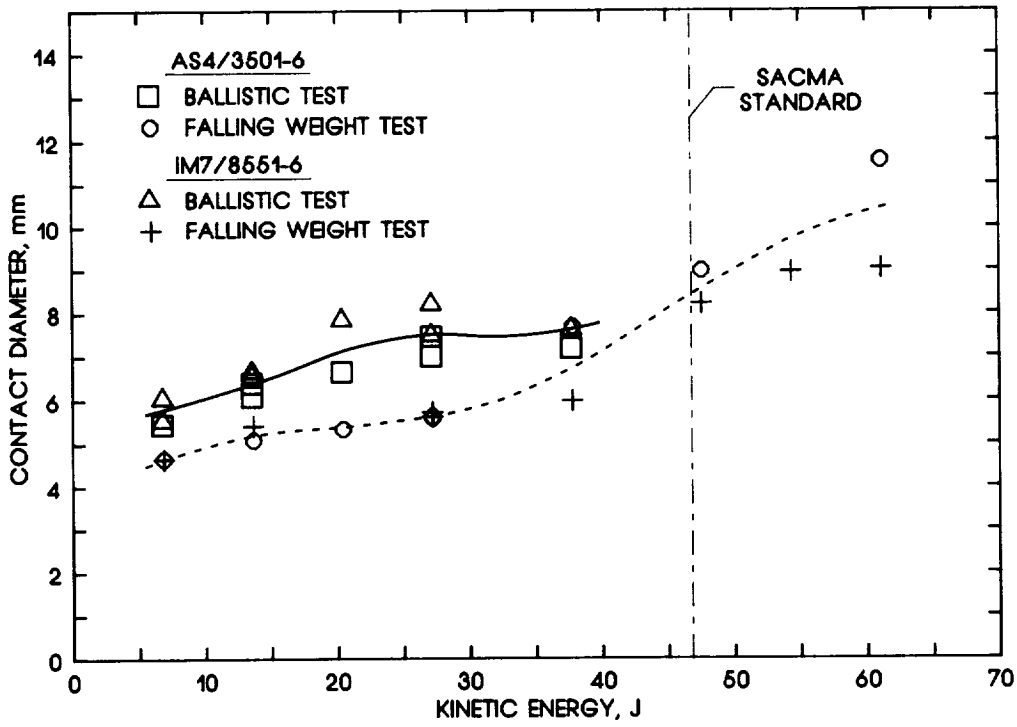

Figure 17.- Contact diameter versus kinetic energy for $[45/0/-45/0/90]_{6s}$ tape laminates.

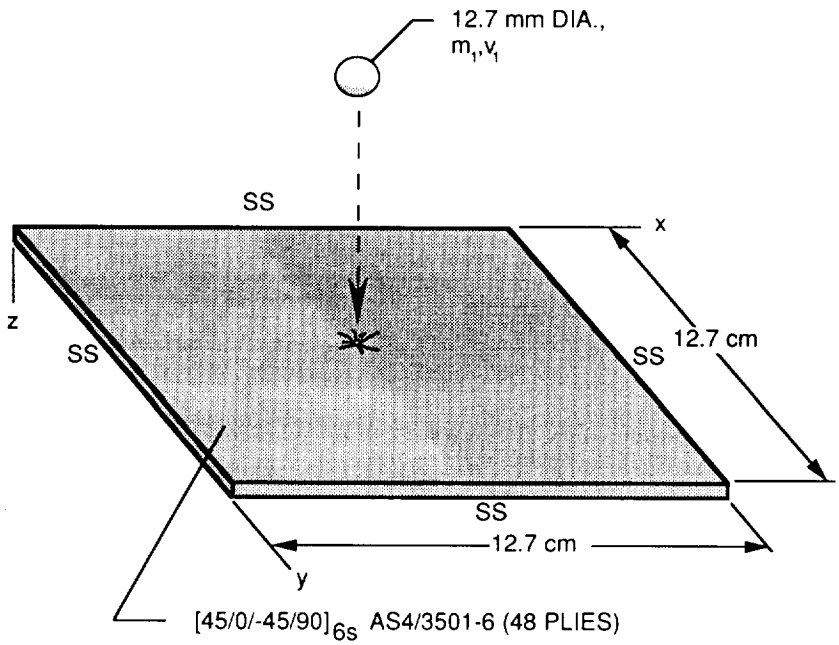

SS -- SIMPLY SUPPORTED

Figure 18. - Plate for impact analysis

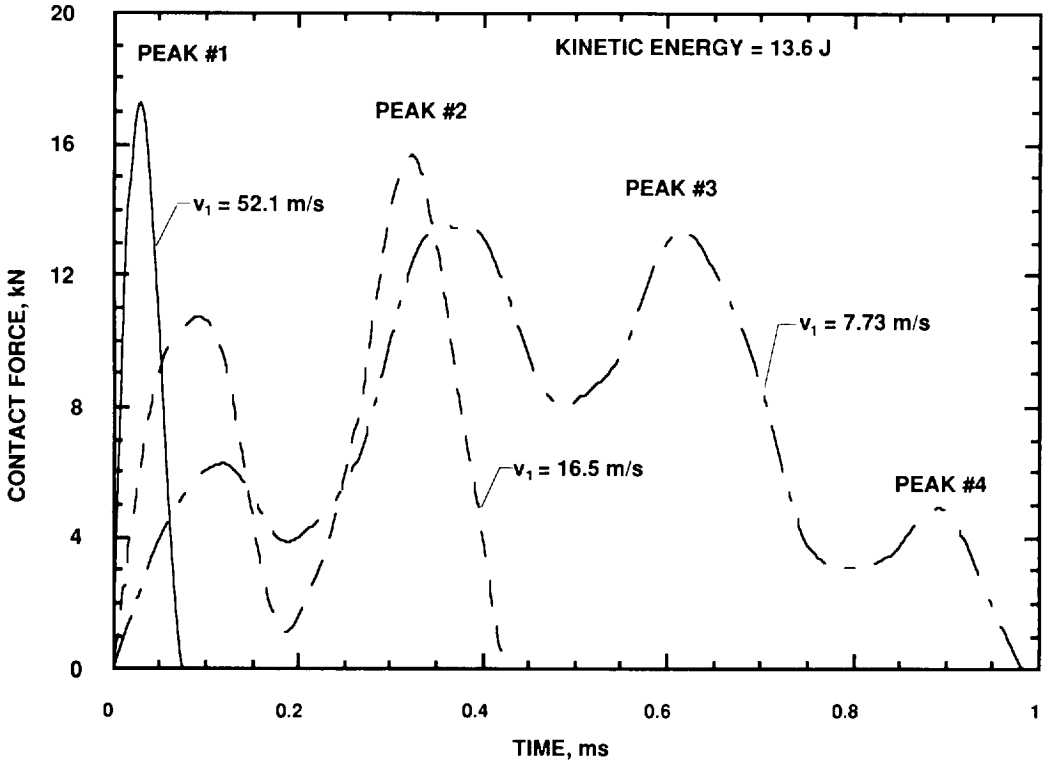

Figure 19.- Predicted effect of velocity on contact force history.

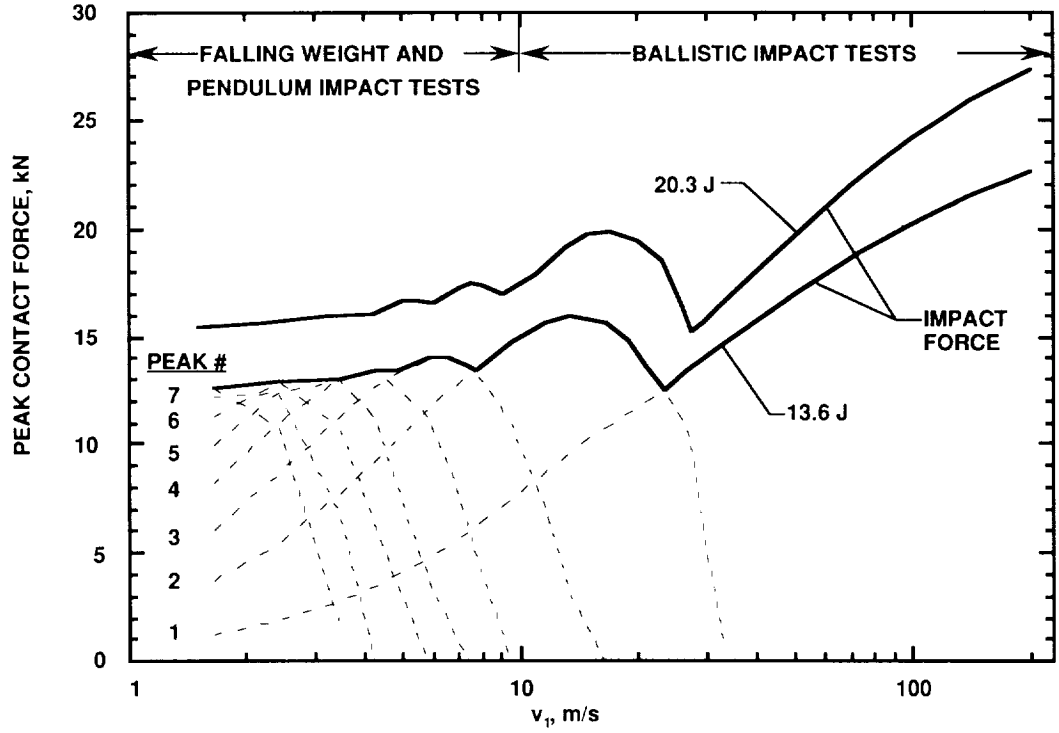

Figure 20.- Predicted peak force versus impacter velocity.

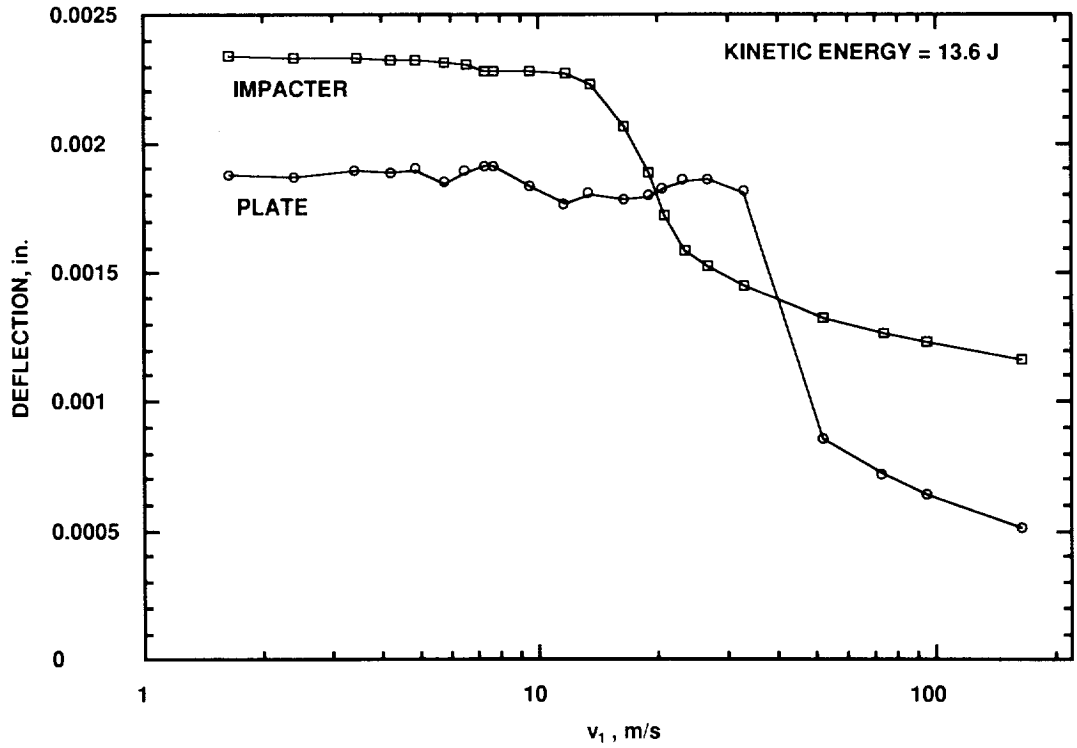

Figure 21. Predicted maximum deflection at center of plate versus impacter velocity.

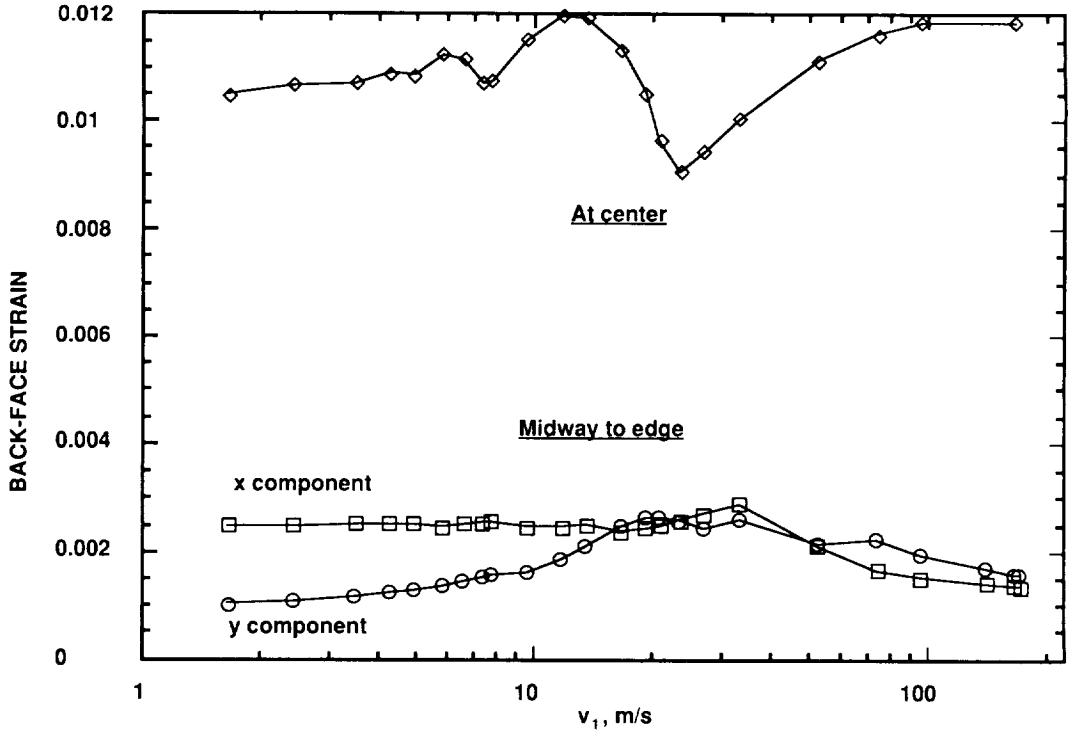

Figure 22.- Back-face strain versus velocity for a kinetic energy of 13.6 J.

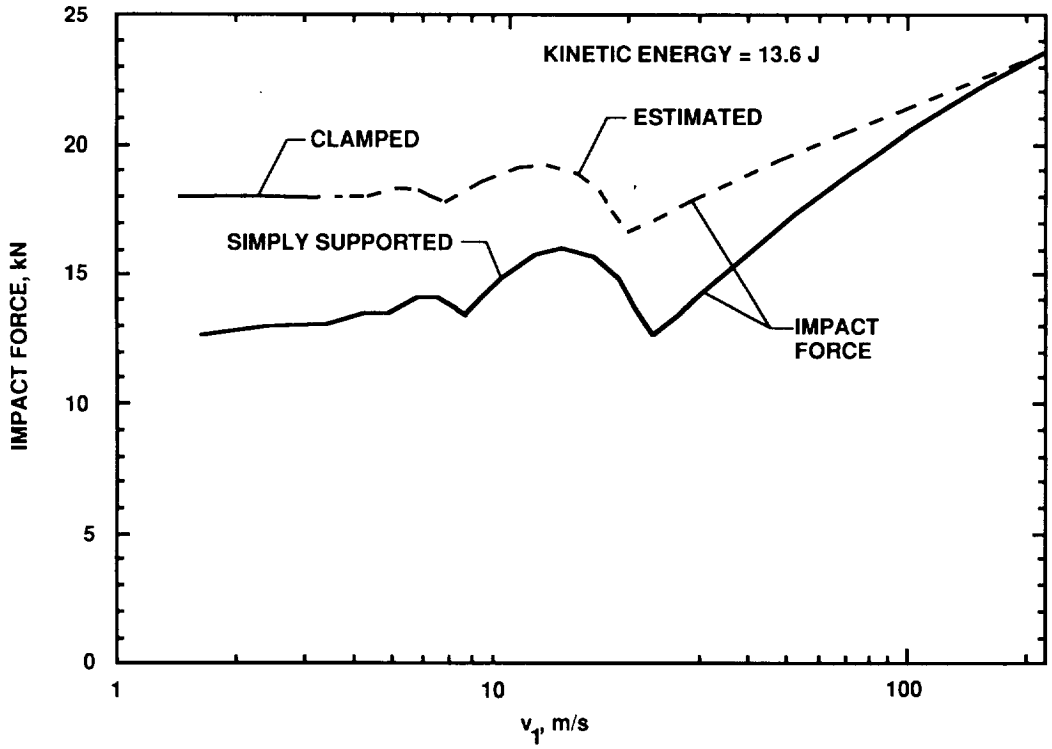

Figure 23.- Predicted impact force versus impacter velocity.